Polyelectrolyte Multilayers (PEM) in Micro / Nanofluidics for Novel BioMEMS Platforms

by

Hongchul Jang

Bachelor of Engineering in Chemical and Biological Engineering
Korea University, South Korea, 2001

Master of Science in Chemical Engineering
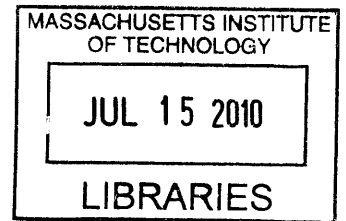Yale University, 2004

**Submitted to the Department of Civil and Environmental Engineering
and the Department of Mechanical Engineering
in Partial Fulfillment of the Requirements for the Degree of**

**Master of Science in Civil and Environmental Engineering
and
Master of Science in Mechanical Engineering
at the
Massachusetts Institute of Technology
February 2010**

Signature of Author: ....
Department of Civil and Environmental Engineering
Department of Mechanical Engineering
January 15, 2010

Certified by: ....
Roman Stocker
Associate Professor of Civil and Environmental Engineering
Thesis Supervisor

Certified by: ....
Roger D. Kamm
Professor of Mechanical Engineering and Biological Engineering
Thesis Co-Supervisor

Accepted by: ....
David. E. Hardt
Professor of Mechanical Engineering
Chairman, Departmental Committee for Graduate Students

Accepted by: ....
Daniele Veneziano
Professor of Civil and Environmental Engineering
Chairman, Departmental Committee for Graduate Students

Polyelectrolyte Multilayers (PEM) in Micro / Nanofluidics for Novel BioMEMS Platforms

by

Hongchul Jang

Submitted to the Department of Civil and Environmental Engineering
and the Department of Mechanical Engineering on January 15, 2010
in partial fulfillment of the requirements for the
Degree of Master of Science in Civil and Environmental Engineering
and Master of Science in Mechanical Engineering

ABSTRACT

The overall goal of this thesis was to exploit the versatility of the polyelectrolyte multilayer (PEM) to fabricate a novel micro/nanofluidic device for patterning bacteria in BioMEMS. Nanofluidic channels offer new opportunities for advanced biomolecule manipulation and separation science because they provide unique capabilities such as ion-permselectivity and nanometer-sized structures. In order to establish industrial applications for biotechnology and medicine, including separation of biomolecules, drug delivery, and single molecule detection, however, regular planar nanofluidic channels have limited fluidic conductance that results low throughput. Therefore, it would be important to develop a robust engineering platform with precise control of depth to the nanometer scale without channel collapse. Nanochannel-induced fluidic conduction can be enhanced by controlling the channel gap size for increasing electrical double layer (EDL) overlap as well as fabricating high-throughput vertical nanofluidic channels. We have fabricated a vertical nanofluidic channel by anisotropic etching of silicon. The gap size of the vertical nanochannel was as low as 50 nm, as obtained by layer-by-layer deposition of polyelectrolyte. Silicon-to-glass bonding was achieved by electrostatic interaction at lower temperature (180 °C) than conventional anodic bonding temperatures (300~400 °C), and even at room temperature (25 °C). The second part of this thesis focuses on patterning bacteria on polyelectrolyte multilayers. Patterns of bacteria are of growing interest in biofilm formation and the broader area of microbial ecology. A simple method to create functionalized surfaces for efficient micro-patterning of bacteria is presented, based on the use of micromolding in capillaries (MIMIC) of poly(ethylene glycol)-poly(lactide) diblock copolymer (PEG-PLA) onto

polyelectrolyte multilayers. Two different implementations showed excellent selective anti-biofouling results for micropatterning of bacteria.

Thesis Supervisor : Roman Stocker
Title: Associate Professor of Civil and Environmental Engineering

Thesis Co-Supervisor : Roger D. Kamm
Title: Professor of Mechanical Engineering and Biological Engineering

Acknowledgements

I would like to extend my sincere thanks and profound sense of gratitude to my supervisor Professor Roman Stocker for his intellectual guidance and constructive criticism. He is a fantastic mentor and a constant source of inspiration. It has been my great honor to work under his guidance.

Professor Roger Kamm, I always remember his generosity and kindness. I would like to thank him for his helpful suggestions and guidance.

I have also appreciated Professor Jongyoon Han for his advice and guidance in the early stages of this research.

I have benefited greatly from my association with all past and present members of the Stocker lab, in particular Marcos, Tanvir Ahmed, Mack Durham, Michael Barry, Mitul Luhar, Dr. Justin Seymour, Dr. Kolja Kindler, Alberto Leombruni, Xavir Corino.

I also warmly thank all present and former members of the Han laboratory. I especially express my gratitude to Dr. SungJae Kim for introducing me to nanofluidics, Dr. Junghoon Lee for fruitful discussions, Dr. Pan Mao for assistance in the fabrication process. I acknowledge the CMSE at MIT for the financial support of my research. I also would like to express many thanks to my friends and colleagues for making my life at MIT special and enjoyable.

Finally, I owe my deepest gratitude to my parents and family who have provided me with great opportunities, everlasting support, and big encouragement.
Most importantly, I would like to give my special thanks and love to my wife Sujin Kim and my daughter, Ashley Chelyn Jang for all the love, support and encouragement. They have been a source of inspiration and this work is a tribute to them.

Hongchul Jang
January 2010

Contents

List of Figures

List of Tables

Chapter 1. Introduction and Background

1.1. Microfluidics

Microfluidics refers to devices and methods for controlling and manipulating fluid flows with length scales less than a millimeter. Such methods have gained tremendous success over the past decade in areas including microelectronics, analytical chemistry, drug discovery, genomics, proteomics and tissue engineering, as well as other biological applications. Microfluidic devices offer significant advantages compared to traditional technologies, including huge decease in reagent consumption, lower cost, smaller overall size, faster processes, better separation resolution, portability, and disposability[1]. Microfluidics utilizes many different components such as valves, pumps, sensors, mixers, filters, separators, heaters etc. These are combined into a micro total analysis system (μTAS, also called 'Lab-On-a-Chip') in which one tries to do such things as chemical synthesis, analysis, and reactions by using very small fluid volumes.

Manipulation of microfluidic flows can be achieved by using different external fields (pressure, electric, magnetic, capillary, etc.). The manipulation can be achieved by either applying the external field at inlets and outlets, or it can be applied locally in the microchannel by integrated components.

1.2. Nanofluidics

Nanofluidics can be defined as the study and application of fluid flow in and around nanometer-sized objects with at least one characteristic dimension below 100 nm. The rationale for moving down the scale from microfluidics to nanofluidics comes from the need to approach the molecular level (1~10 nm) in order to understand many fundamental biological processes, such as translation, gene regulation, mitosis, and cell communication[1]. Availability of nanofluidic tools with a similar size dimension as the target biomolecules and organelles will allow better manipulation of these systems in general. There is a great deal of information about the mechanisms behind biomolecular activities that can only be uncovered by studying single molecules, which is conceivable with the development of nanofluidic tools. Understanding molecular transport will reveal new research thrusts, such as single molecule sequencing and molecular separation. In addition, nanofluidic tools could be significant due to the promise of the discovery of new phenomena, not occurring at micro or macro scales. Thus, there is ample motivation to explore molecular transport in nanoscale structures.

It is now feasible to fabricate nanofluidic channels with truly molecular dimensions, down to a few nanometers[2], using only standard microfabrication techniques[3]. This opens up a new possibility of using regular-shaped nanochannels in lieu of random nanoporous membranes, only with a better knowledge and control of the pore characteristics. Recent engineering examples include the separation of biomolecules such as DNA and proteins[4-5], as well as nanofluidic preconcentration systems[6] shown in Figure 1-7. In addition to various applications[4,6-10], nanofluidic channels can be an ideal, well-controlled experimental platform to study nanoscale molecular/fluidic/ionic transport properties.

15
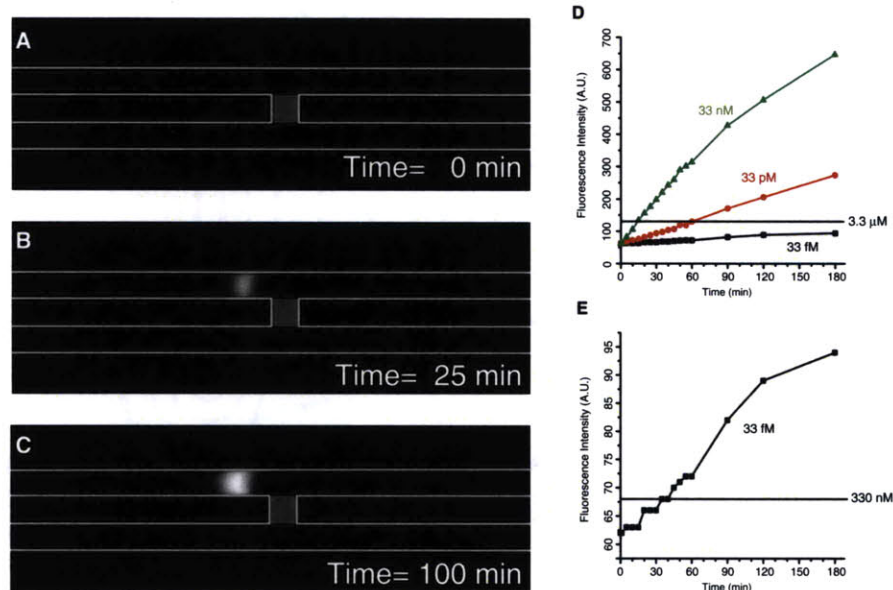
Figure 1-1 Ion preconcentration using planar nanochannels (A) Image of 33 pM protein directly after loading the sample into the top microfluidic channel. (B) Image after applying the electric field for 25 min and (C) after 100 min. (D) Concentrations of the collected protein plug, for three different concentrations. (E) Closeup view for the 33 fM protein experiment. This shows at least 10^7-fold concentration achieved within 40 min, from Wang et al[11].

1.3. **Layer-by-Layer Polyelectrolyte Multilayers**

As a means to produce ultrathin organic films, polyelectrolyte multilayers (PEMs) formed by layer-by-layer deposition have received much interest for the simplicity of processing and versatility of applications. Since Decher et al[12-15]. triggered the practical use of sequential adsorption of oppositely charged polyelectrolytes, numerous studies[16-18] have contributed to rapid growth of this particular technique.
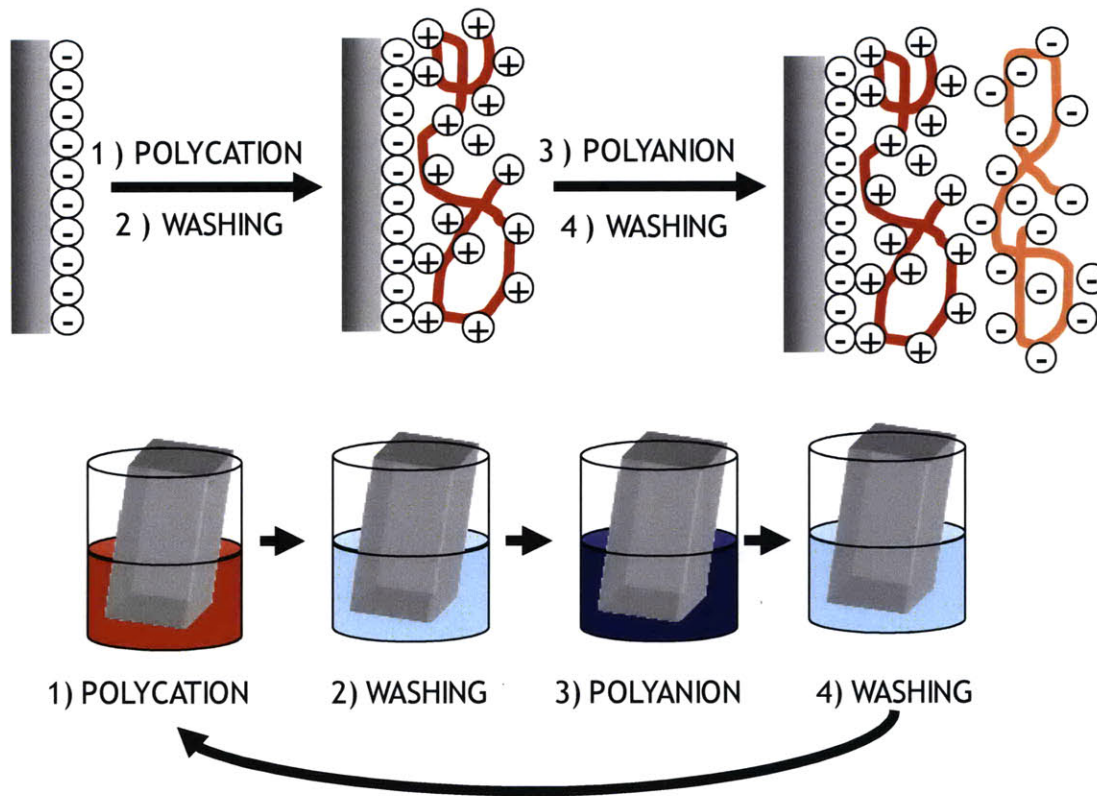
Figure 1-2 Assembly process for layer-by-layer polyelectrolyte multilayer films formed by alternately dipping a substrate in a polycation and a polyanion solution.

The basic mechanism of the layer-by-layer deposition technique is the strong electrostatic attraction between oppositely charged molecules. Figure 1-2 depicts the scheme of electrostatic layer-by-layer self-assembly[16]. When a charged substrate is immersed into a polyelectrolyte solution of the opposite charge, chains in the solution adhere to the substrate surface to neutralize the surface charge leading to overcompensation[19]. Due to electrostatic repulsion between molecules of the same charge, the adsorption process is self-limited to one monolayer. The surface charge is now reversed[20-21], and this enables the next step where oppositely charged molecules adsorb onto the previous layer again reversing the surface charge. By repeating these

alternating deposition steps, polyelectrolyte multilayers can be made as thick as desired.

This simple characteristic of layer-by-layer deposition opens a big window for candidate materials that can be processed via this method. Charged polymers used for PEM assembly are classified as strong or weak polyelectrolytes based on their ionizable charged groups, as shown in Figure 1-3.
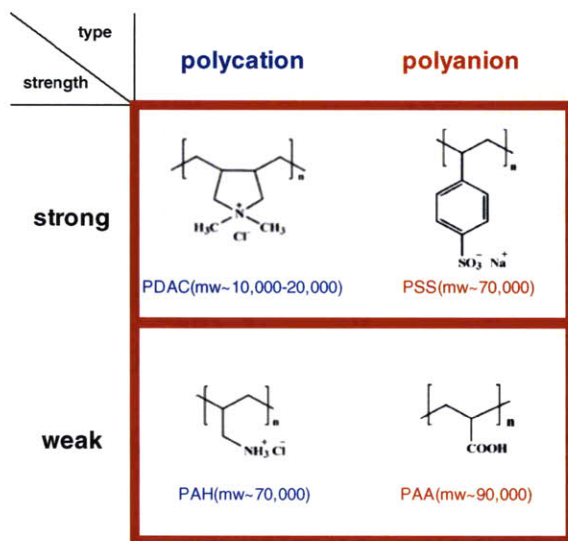
Figure 1-3 Chemical structures of commonly used strong and weak polyelectrolytes. mw is the molecular weight.

Those polymers that maintain a fixed charge over a broad range of pH conditions are termed *strong polyelectrolytes*. In contrast, the degree of ionization of weak polyelectrolytes, such as poly(allylamine hydrochloride) (PAH) and poly(acrylic acid) (PAA), is highly sensitive to the local pH. Polyelectrolyte multilayers made from weak polyelectrolytes have the advantage that their properties can be tuned by simple pH adjustments.

Rubner and coworkers[22-23] performed extensive studies of the structure and properties of weak polyelectrolyte multilayers built via layer-by-layer deposition. Their results (Figure 1-4) show how the bilayer thickness dramatically changes depending on the pH combination of

18

polyelectrolyte dipping solutions. It was found that the internal structure and the surface characteristics of multilayer platforms are determined mostly by the pH conditions of the polyelectrolyte solutions during the dipping process.
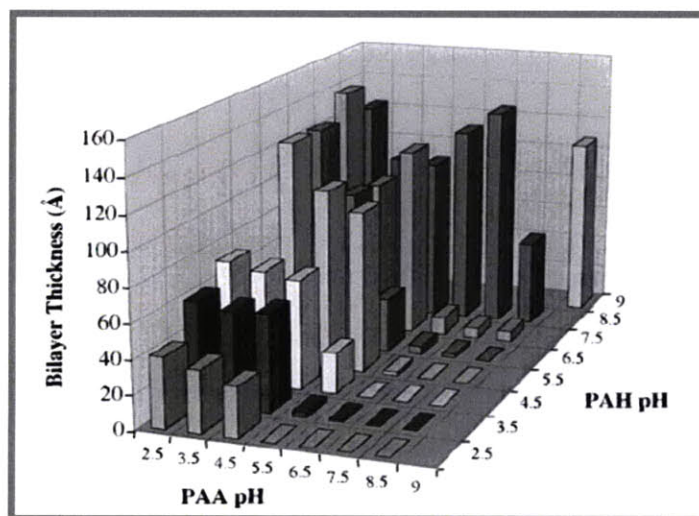
Figure 1-4 pH matrix showing the average incremental thickness contributed by a PAH/PAA bilayer as a function of the pH of the dipping solution. Adapted from the work Shiratori et al[23].

The common notation used to describe assembled PEMs is *(poly1 / poly 2)_x pH1 / pH2*, where *poly1* and *poly2* are the polymers used and *pH1* and *pH2* are the respective pH conditions at which those polymers were adsorbed. *x* is the number of bilayers, where one bilayer consists of one adsorption of *poly1* and one adsorption of *poly2*.

PEM film thickness is highly tunable. Multilayer buildup can proceed in a linear or exponential fashion, depending on the polymer system chosen. Bilayer thickness can be varied by manipulating assembly conditions such as pH and ionic strength. Total film thickness can be adjusted by controlling the number of bilayers. From the collective survey of the pH assembly combinations in Figure 1-4, three different pH systems that represent the unique assembly

mechanism of weak polyelectrolyte multilayers process in each regime are selected for further investigation, specifically pH 6.5/6.5, pH 2.5/2.5, and pH 7.5/3.5. A schematic of the molecular structures in each pH system is shown in Figure 1-6.

| Inertial thin flat layer | Internal active layer | Outermost active layer |
| pH (PAH/PAA): 6.5/6.5 | 2.5/2.5 | 7.5/3.5 |
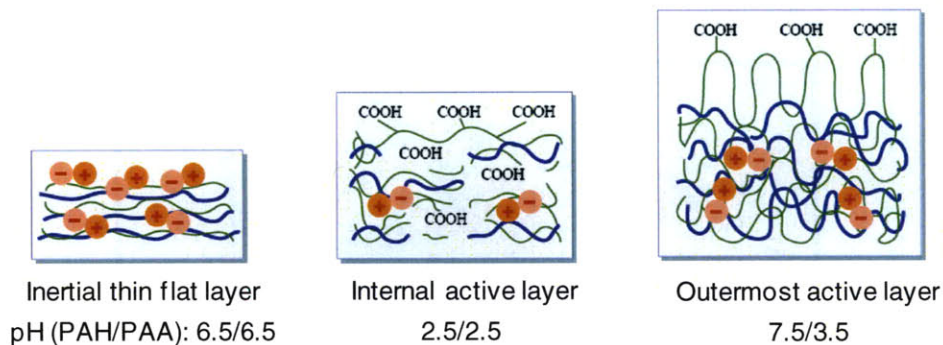
Figure 1-5 Schematic of the surface of PAH/PAA multilayers with PAA as the outermost layer at different assembly PAH/PAA pH's.

Due to the nature of the PEM assembly process, PEMs can be adsorbed onto a variety of substrates with differing geometries. Glass slides, polystyrene tissue culture dishes, fabrics, and PDMS are common substrates used. Once assembled, PEMs are stable with respect to moderate pH and ionic strength and ethanol treatment for sterilization.

For low molar-mass weak acids or bases, the ionization behavior is explained by the Henderson-Hasselbalch equation:

$$pH = pK_a + \log\frac{\alpha}{1-\alpha} \qquad (1.1)$$

where pK_a is the dissociation constant of the weak acid, and α is the degree of ionization.

In the case of low molar-mass weak acids, pK_a remains close to the intrinsic ionization constant (pK_0), with only a slight increase over a large range of α. However, for weak polyacids in solution, as the degree of ionization increases, removing a proton from a new acid group on the

chain needs extra work (ΔFe), due to the electrostatic resistance of the neighboring negative changes that are previously formed[24-25]. Hence, the effective pK_a of weak polyacids depends rather significantly on the degree of ionization. In fact, theoretical calculation predicted the effects of degree of ionization on the apparent pK_a in weak polyelectrolytes to shift the pK$_a$ values by 0.96 pH units from zero ionization to 100% ionization in the absence of salt, and the empirical data of PAA titration showed a large pK_a value of 2.5 pH units in the absence of salt. The detailed acid-base chemistry is described in Appendix A.

1.4. Motivation and Scope of the Thesis

Recently, the science and engineering of molecular transport within nanofluidic channels, with critical dimensions of 10-100 nm, have drawn much attention due to significant advances in micro-/nano-fabrication techniques[3]. While nanochannels are a good model system for studying molecular dynamics in confined spaces, and have achieved great success in biomolecular separation, higher fluidic conductance would be preferred for many applications, including high-throughput molecular sorting, filtration and separation. To obtain large cross-sectional areas in the nanofluidic regime for high ion-selective throughput, thin long channels are required. However, considering the strong electric field and high temperature used in the bonding process, the channel might sag or collapse, changing the channel depth. Thus, developing a new, low-temperature bonding method that avoids shape distortion is a major challenges in the fabrication of micro/nanofluidic devices.

In BioMEMS, the technique of selective immobilization of cells in defined positions or areas using a precise understanding of the interactions between cells and surfaces is essential for

important applications such as biosensors, biochips, biomedical microdevices, and tissue engineering. However, conventional surface modifying techniques are costly and afford only a narrow window for the choice of the chemicals. To minimize cell adhesion (e.g. for implant applications) or to better control surface properties, polyelectrolyte multilayers can be excellent candidates, because (i) the versatility of the multilayer formation process with respect to the variety of materials which can be used as building blocks, and (ii) the possibility of combining this with other assembly procedures, result in high application potential in a broad range of different areas of materials development.

Engineering extremely perm-selective membranes by the synergism of nanofluidics and polyelectrolyte multilayer (PEM) for applications ranging from preconcentrator to fuel cell has gained increased emphasis. However, a robust platform that can account for increasing electrical double layer overlapping effects, achieving low temperature bonding without collapse of channels, and proving an easy process for surface modification on demand have yet to be developed. This thesis aims to improve current nanofluidic devices, especially producing massively-parallel, regular vertical nanochannels with a uniform, well-controlled gap size of ~50 nm for high-throughput membrane applications. As can be seen in Figure 1-6, the approach of polyelectrolyte multilayer (PEM) on a chip developed in this thesis could be of benefit. The PEM deposition step serves three purposes. Firstly, it is to build high-aspect-ratio (ratio of depth to width) vertical nanochannels by the control of the lateral gap size. The gap size can be controlled with nanometer-scale by the technique. Secondly, PEM offers electrostatic low temperature bonding with keeping channel dimensions uniform. Finally, it is capable of controlling the topographic organization of the films by micropatterning, which provides insights into to mechanisms underlying cell/surface and cell/cell interactions.

22
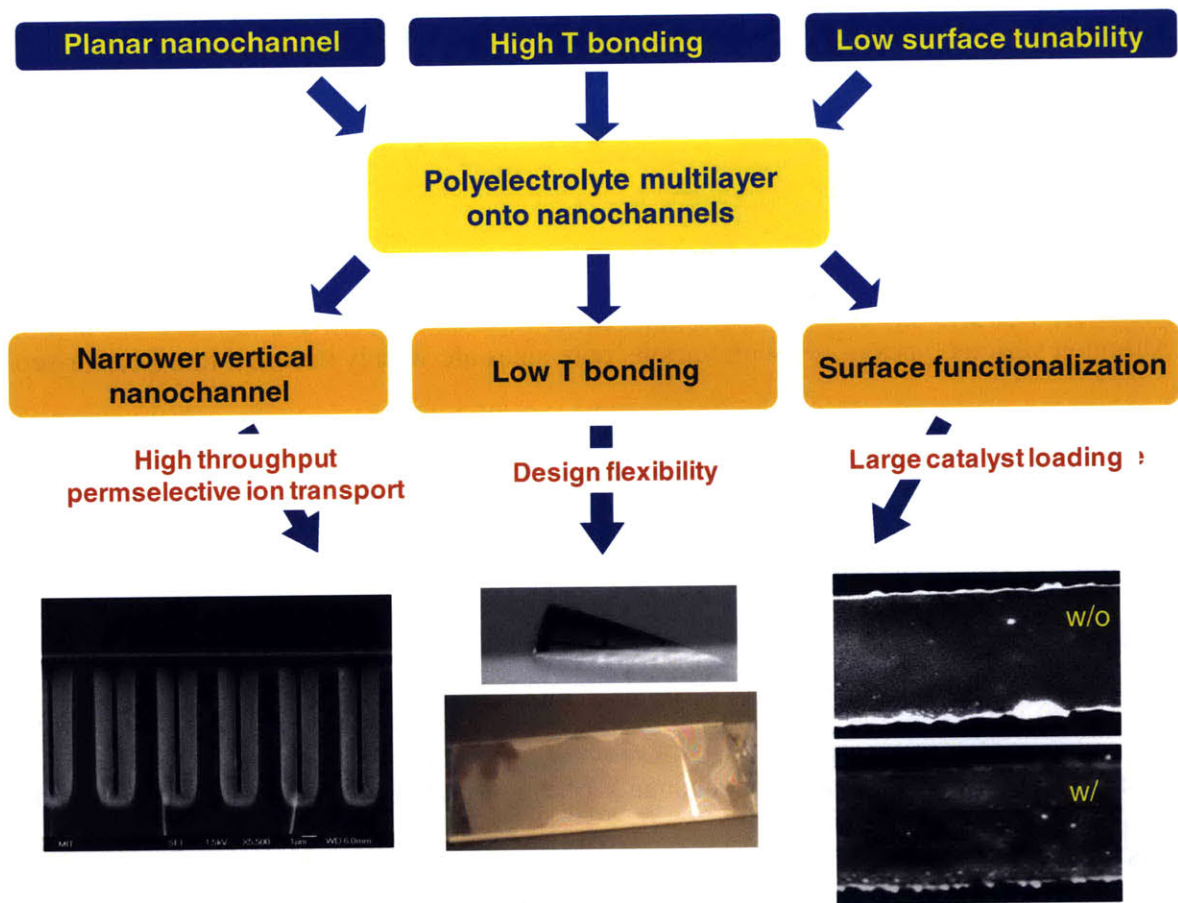
Figure 1-6 Schematic overview of polyelectrolyte multilayer application in BioMEMS.

Chapter 2. Fabrication of Micro/Nanofluidic Channels

2.1. Introduction

Although various types of gel with various pore sizes are widely used in biomolecular separation, investigating transport through nanoporous systems is challenging due to the geometry and surface condition of nanopores of gels, characterized by parameters such as pore length, deviation of pore shape from perfect cylinders, and pore size distribution, which are difficult to deduce and control[26].

In order to overcome the limitations of nanoporous gels, solid-state nanometer-sized structures are required. Micromachined nanochannels offer unique advantages over random nanoporous gels because their geometry and surface properties can be well defined in order to model transport through nanochannels or study molecular dynamics in confined spaces.

This chapter presents the fabrication of solid-state nanochannels on silicon and glass substrates and bonding processes to achieve enclosed systems. Various methods of producing nanochannels exist and are divided into the categories of *top-down* and *bottom-up* fabrication methods[27]. We focus here on the well-established *top-down* processes for the fabrication of channels with the smallest dimension below 100 nm. The design of the micro- and nanochannels on chip is shown in Figure 2-1.

24
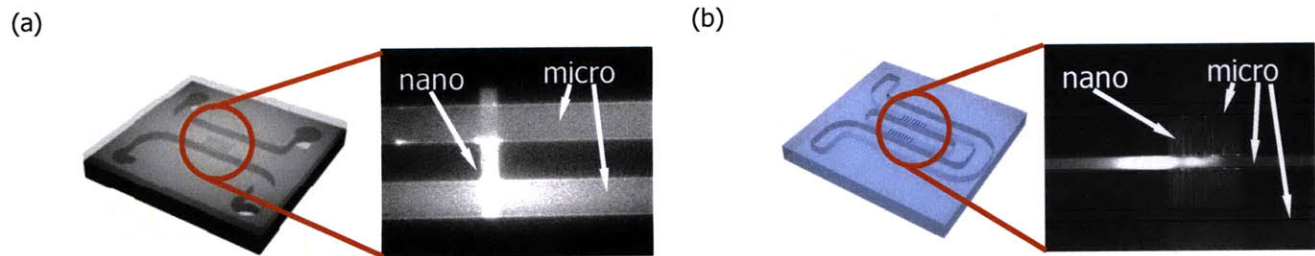
Figure 2-1 Schematic configurations and microscopic images of (a) Single nanochannel bridge device on silicon substrate and (b) Dual nanochannel bridge device on glass substrate.

2.2. **Micro/Nanochannels on Silicon Substrate**

A schematic diagram of the fabrication process is given in Figure 2-2. First, silicon wafers were cleaned in a piranha solution (H_2SO_4 (%): H_2O_2(%) = 3:1) for 10 min, rinsed in DI water and spun dry with nitrogen gas. Then, nanofluidic channels with various widths and depths were patterned and etched into silicon wafers by using standard photolithography and reactive ion etching (RIE) techniques. It is straightforward to control the depth of the channel, since the etch parameters can be controlled easily. After residual resist removal, the etched depth was measured with a surface profilometer (Prometrix P-10, KLA-Tenco Co., CA.). Then, a standard photolithography process was performed again on the wafer with a photomask having the patterns of microchannels. The microchannel was also etched using RIE techniques. After patterning of the channels, a potassium hydroxide (KOH) etching technique was used to make access holes from the backside of the wafer. After thermal oxidation for electrical insulation, the silicon chip was bonded with a flat glass plate (Pyrex Corning 7740 or Borofloat, Sensor Prep Services, Inc., IL) by anodic bonding technique. The bonding process was carried out at 350 °C with an applied voltage of 800 V in the bonder machine (EV501, Electronic Vision group). All

25

the fabrication process, except bonding, was done in the MTL cleanroom at MIT. The detailed process flows are described in the Appendix B-1.
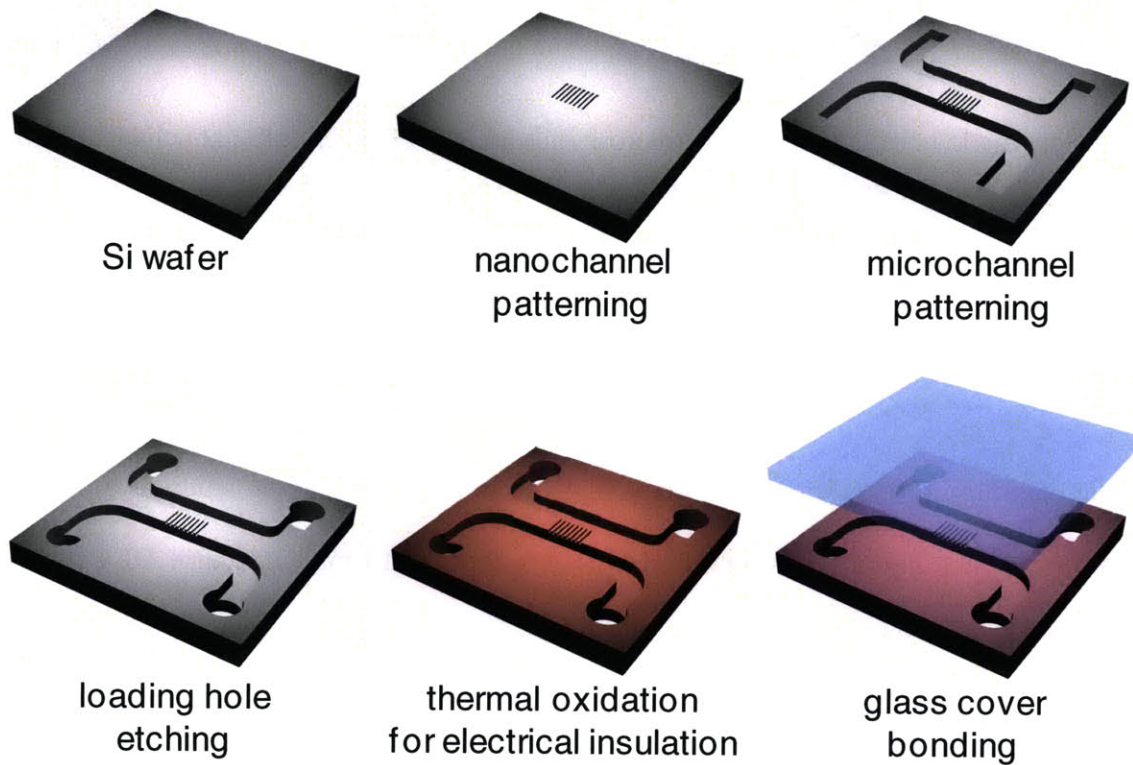
Figure 2-2 Fabrication process of nanofluidic channels on silicon substrate

2.3. **Micro/Nanochannels on Glass Substrate**

The nanochannel chip described in Figure 2-3 was fabricated on two pyrex wafers with a diameter of 150 mm and a thickness of 0.5 mm. The top wafer has reservoirs (1 mm diameter) that were fabricated using an ultrasonic drilling system by Sensor Prep Services. The bottom wafer contains both micro and nanochannels. The fabrication process of channels is as follow. The glass wafers were cleaned in a piranha solution (H_2O_2 and H_2SO_4, 75 ml and 225 ml,

respectively) for 10 min, rinsed in DI water three times and spun dry with nitrogen gas. To remove adsorbed water at the glass wafers, a dehydration bake of the surfaces was performed at 120 °C for 30 min in a convection oven. The wafers were vapor-primed with adhesion promoter, hexamethyldisilazane (HMDS), in a vacuum chamber followed by spin coating with an OCG 825 as positive photoresist and soft baking at 95 °C for 30 min in a convection oven to remove solvents and stress for increasing adhesion of the resist layer on the wafers. A standard photolithography process was performed on this photoresist layer with a photomask having the patterns of the nanochannels. After developing in OCG 934 1:1 developer, de-scumming was conducted at 1000 W for 5 min in oxygen plasma chamber to remove unwanted resist left behind after development. Hard baking at 120 °C for 30 min in a convection oven was performed before etching the wafers by immersing in a commercial buffered oxide etchant (BOE 7:1), without agitation. After residual resist removal, depth measurement of the fabricated channels was performed with P-10. Then, a 20 nm chromium layer and a 100 nm gold layer were successively deposited on the wafers using an evaporator. Following same processes described above, the patterns of the microchannels were transferred onto the pyrex surfaces after etching the gold and chromium with gold etchant (Aqua Regia, 3:1 HCl:HNO$_3$) for 30 s and chromium etchant (CR-7) for 25 s. Microchannels were etched by dipping in an HNA (650 : 150 : 200, DI water : HNO$_3$: HF) bath. The etch rate was 0.8 μm/min. Finally, residual photoresist, gold, and chromium layer were removed using acetone, gold, and chromium etchant, sequentially. The etched glass substrate and the cover glass that had the loading hole were bonded by thermal fusion bonding. The important factors affecting successful thermal fusion bonding of glass chips include the cleanliness of the bonding glass surface, the surface flatness of glass substrates, the bonding temperature, and the pressure. Therefore, the substrate and the cover glass were cleaned in

piranha solution for 15 min and then activated with 28% ammonium hydroxide at 50 °C for 30 min. After spinning dry, the two glass wafers were carefully aligned and pressed together to make a spontaneous bonding with about 5 lb of weight (metal plate) for a couple of hours or overnight, prior to the thermal bonding process. Then, annealing was performed by fusing the two glass wafers in a programmable furnace (Model BE51894C-1, Lindberg/Blue M, NC) at 550 °C for 12-15 hours with a ramp rate of 1.5 °C min^{-1} and a cool-down rate of 2.5 °C min^{-1}. The detailed process flows are described in the Appendix B-2.

glass wafer   nanochannel patterning

microchannel patterning   glass cover bonding
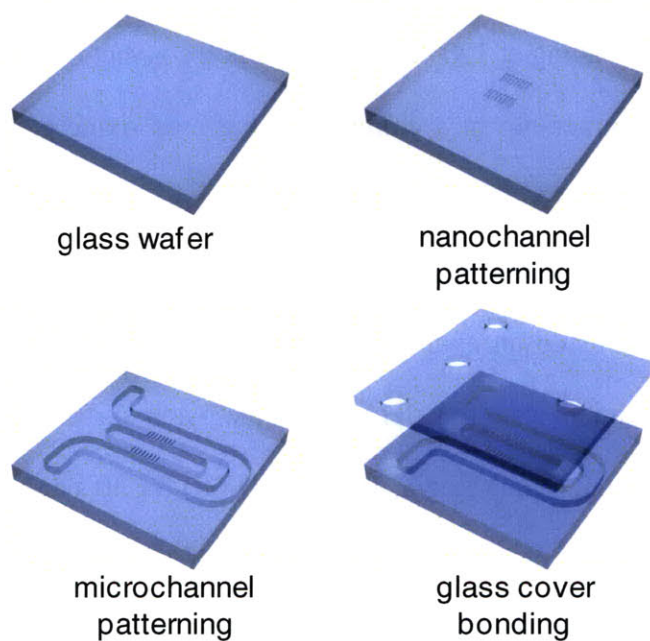
Figure 2-3 Fabrication process of nanofluidic channels on glass substrate

2.4. **Summary**

In summary, we can fabricate regular "thin" planar nanofluidic channels on both silicon and glass substrates using standard photolithography techniques. The technique is simple and repeatable, and nanochannels made by this method are mechanically robust. The fabrication on glass was much simpler than on silicon. When using a glass chip, we can expect the perfect plug type flow pattern due to the same surface potential at the walls of the glass chip. While the "thin" planar nanochannels are a good model system for studying molecular dynamics in confined spaces, higher fluidic conductance would be preferred for the applications of high-throughput molecular sorting, filtration and separation. One approach to generate deep massively-parallel vertical nanochannels with good control of lateral gap size of the channels using polyelectrolyte multilayers (PEMs) is described in Chapter 3.

Chapter 3. Polyelectrolyte Multilayer for Controlling Gap Size of Vertical Nanochannels

3.1. Introduction

Although it is now possible to fabricate a regular "thin" nanofluidic channel with uniform thickness, a critical issue in nanofluidics is the reliable, reproducible fabrication of nanometer-sized fluidic structures with high throguhput as large as standard microfluidic channels for efficient molecular separation and manipulation. Figure 3-1 shows the conceptual comparison of planar nanochannels and vertical nanochannels. The cross-sectional flow area (open pore volume per unit length) of the vertical channels can be more than hundred-fold higher than the cross-sectional area of the planar channels. Therefore, the sample throughput (volume flow rate) of the vertical system can be up to three orders of magnitude higher than the throughput of the planar system with a similar flow velocity, while they possess similar device characteristics due to the same critical dimension[28].
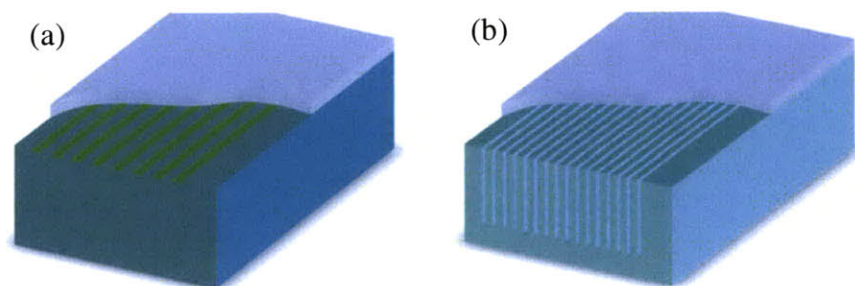
Figure 3-1 Cartoon illustrates the comparison of (a) planar (low-aspect-ratio) nanochannel system and (b) vertical (high-aspect-ratio) nanochannel system. They both have the same critical

dimension (depth for planar channels and width for vertical channels) but the open volume of vertical channels can be a few orders of magnitude larger than planar channels, from Mao et al[28].

This chapter describes a method to produce massively-parallel, vertical nanochannels with good control of the channel gap size using polyelectrolyte multilayers as well as to fabricate high-throughput vertical nanofluidic channels for enhancing nanochannel-induced fluidic conductance.

3.2. Fabrication of Vertical Nanofluidic Channel on Silicon

Since the overall fluidic conductance of the planar nanochannels is limited compared with more traditional membrane materials such as gels, massively-parallel nanofluidic channels with fluidic conductance as large as standard microfluidic channels would be highly desirable for efficient molecular separation and manipulation applications. To obtain high throughput, we fabricated vertical nanochannels with high aspect ratio as shown in Figure 3-2.

(a)

1. LPCVD nitride deposition
2. Photolithography and RIE silicon nitride etching
3. DRIE or KOH etching
4. Silicon nitride removal
5. Thermal oxidation

Si(110) substrate

(b) Before Oxidation (~**1100nm**)

➤ High aspect ratio vertical nanochannels

(c) After Oxidation (~**350nm**)

➤ **Challenges : Required narrower & uniform nanochannels**
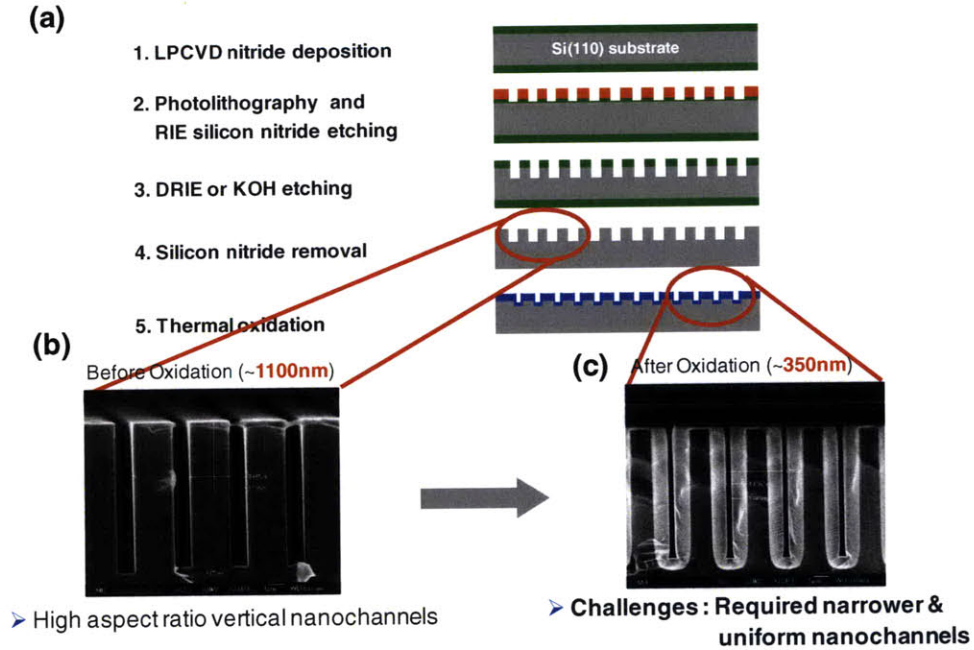
Figure 3-2 (a) Fabrication process of vertical nanochannels with DRIE/anisotropic etching and the cross-sectional SEM images of nanochannels (b) before (~1100 nm) and (c) after (~350 nm) oxidation.

Anisotropic etching of (110) silicon provides an attractive and effective method for fabrication of high aspect-ratio structures with smooth and vertical sidewalls because of the high selectivity between (110) and (111) planes (larger than 100:1). Figure 3-2(b) shows a cross sectional view of a high aspect-ratio channel with a depth of ~10 μm and a width of 1.1 μm. After depositing an oxide layer as an insulator, we took the cross-sectional SEM image as shown in Figure 3-2(c). It shows that vertical nanochannels are 250-350 nm wide. Since the oxidation rate within the vertical channels could be retarded due to hindered transport of oxidizing species[29], the gap size might become non-uniform in very narrow, deep channels. Thus, the control of the uniform gap size by thermal oxidation down to below 100 nm is complicated by the *top-down* method.

3.3. Controlling Gap Size using Polyelectrolyte Multilayer

Narrowing the gap size of nanochannels down to below 100 nm is highly desirable in order to carry out molecular control and manipulation, yet the narrowness of these channels is greatly limited by the deep reactive-ion etching (DRIE) step, which is a highly anisotropic etch process used to create deep, steep-sided trenches in wafers, with aspect ratios of 20:1 or more. Too narrow a trench will create a tapered profile, and also a rough sidewall[29]. The fabrication of narrower and more uniform vertical channels to increase surface effects at the nanoscale can be achieved by polyelectrolyte coating, which is the ideal processing tool to tailor highly perm-selective nanofluidic channels because of its ease of controlling thickness per deposited layer, modulating surface charge density and properties. The formation of self-assembled structures can be considered as a *bottom-up* approach towards formation of nanostructures. Polyelectrolyte multilayers are assembled using a layer-by-layer assembly process that is shown graphically in Figure 3-2. In a typical process, a substrate is dipped into the first polyelectrolyte solution for a long enough time to allow the polyelectrolyte to adsorb to the surface. After rinsing off loosely bound polymer, the substrate is then dipped into a polyelectrolyte solution of opposite charge. This second polyelectrolyte adsorbs to the surface due to electrostatic attraction and actually overcompensates for the surface charge resulting in a reversal of the surface charge. The process is repeated until the desired number of layers is deposited.
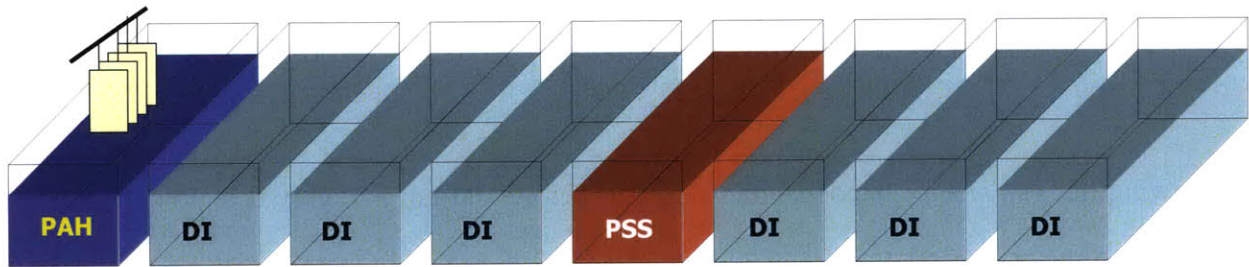
Figure 3-3 Schematic of a dipping technique for fabricating polyelectrolyte multi-layers, poly allylamine hydrochloride (PAH) and poly sodium 4-sty-renesulfonate (PSS).

We have fabricated vertical nanofluidic channels by anisotropic etching of silicon. A gap size of the vertical nanochannels as low as 50 nm was achieved using layer-by-layer deposition of the polyelectrolyte, as shown in Figure 3-3.
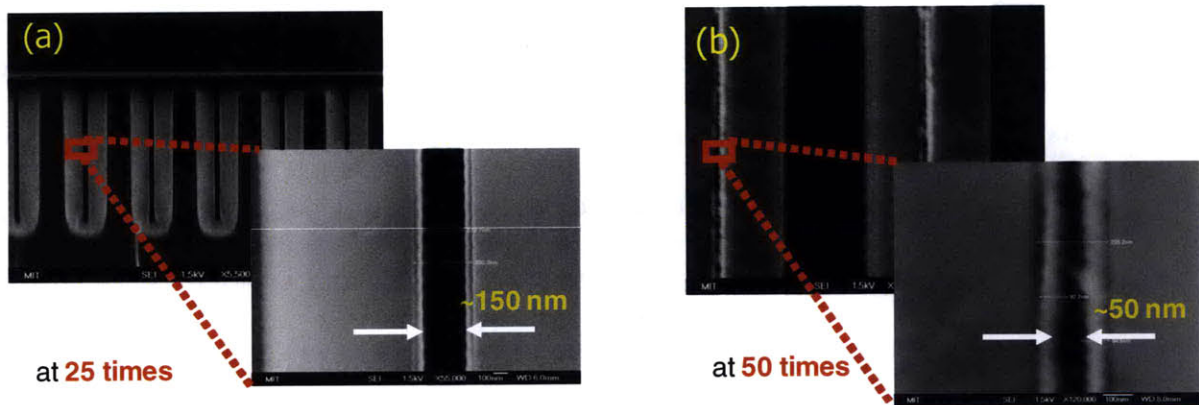
Figure 3-4 SEM images of nanochannel cross-sections after PAH/PSS coating (a) 25 and (b) 50 times. The gap sizes are (a) ~150 nm and (b) ~50 nm.

3.4. Conclusion

We developed a novel fabrication strategy for generating massively-parallel, regular vertical nanochannels with a uniform, well-controlled gap size of ~50 nm, by combining *top-down* and *bottom-up* methods, where the smallest nanostructures achieved by *bottom-up* method can be controlled by layer-by-layer deposition of polyelectrolyte multilayers (PEMs). It is expected that the availability of well-defined high-aspect-ratio nanochannels with good control of channel gap sizes down to near-molecular dimension (10 - 100 nm) will be widely beneficial for research in the biological and biophysical sciences. To keep the uniform gap size along the channels, a new bonding method need to be developed to eliminate the channel collapse or sag resulted from traditional high temperature bonding methods such as anodic bonding and thermal fusion bonding. It is discussed in Chapter 4.

Chapter 4. Polyelectrolyte Multilayer for Substrate Bonding

4.1. Introduction

In this chapter, we see that conventional bonding processes would change the depth of the nanochannels defined in the silicon or glass substrates. Having found the collapsing or sagging of the channel in conventional bonding processes at high temperature, we now present a new easy bonding method employing polyelectrolyte multilayers at low temperature (chapter 4.2).

Silicon-Glass bonding

Typically, anodic bonding requires high temperatures (300-400 °C) and high electric fields (400-1000 V) to generate a permanent bonding between silicon wafer and glass. Generally, the stacked silicon and glass substrates are assembled and heated on a hot plate to high temperature (~350 °C). The bonding method will work only with certain type of glass materials, because of the required thermal matching between Si and glass. Typically borosilicate glass materials (for example, Corning 7740 Pyrex) are well suited for anodic bonding.

Recently, Mao *et al*[30]. established a criterion for the the survival or collapse of nanochannels, in terms of the width and depth of the channel by optical observation. An optical micrograph of the typical success or failure of nanochannels is shown in Figure 4-1. The channels turned from bright to gray when they collapsed. Once its roof makes contact, a channel collapses quickly and completely due to the attractive interfacial surface forces, except the narrow region along the edges.

Maximum critical AR (*w/d*)~250
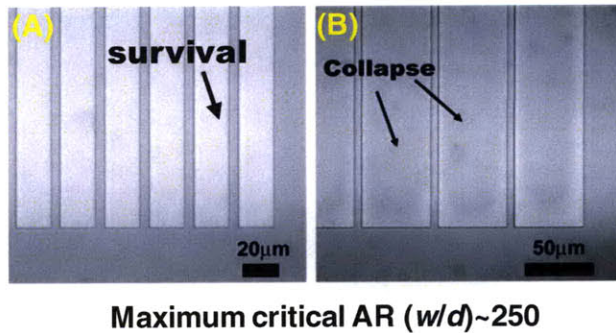
Figure 4-1 Optical observation of the survival or collapse of the channels. (A) Survived channels with the depth of 80 nm and width of 20 μm, spaced by 5 μm. (B) Collapsed channels with the depth of 80 nm and width of 50 μm, spaced by 5 μm. Very small areas along the edge did not collapse. Adapted from the work of Mao et al[30].

The results show that the aspect ratio of the channel (width/depth) is an important factor to determine the success or failure of the fabrication. The maximum aspect ratio of surviving channels is around 250.

Glass-Glass bonding

Thermal fusion bonding at high temperature can provide good bonding strength and high bonding yield. Lin *et al*[31]. succeeded in sealing mcrofluidic channels on soda-lime glass at 580 °C for 20 min with a slight pressure applied. Fan *et al.*[32] achieved effective bonding between two Pyrex glass at 640 °C after 6 hours. Although glass-glass bonding at high temperature (~600 °C for Pyrex) can be achieved successfully with large bonding strengths, the channels tend to be distorted and even collapsed since the glass material at this high temperature will be softened. Figure 4-2 (A) shows the optical image of 25 nm deep channels. This aspect ratio is much larger than the one (~0.004) obtained for silicon-glass channels by using anodic bonding techniques. The optical image of the 15 nm deep nanochannel with a width of 3 μm is shown in Figure 4-2 (B). It can be seen that nanochannels collapsed in some regions but survived in the other regions.

37

Maximum critical AR (*w/d*)~400
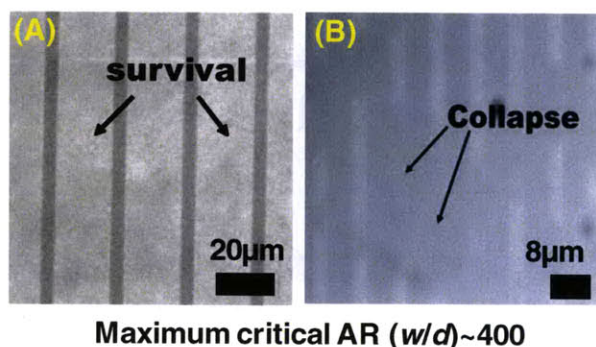
Figure 4-2 Optical micrograph of glass nanochannels. (A) 10 μm wide and 25 nm deep nanochannels survived after bonding. (B) 3 μm wide and 15 nm deep nanofluidic channels collapsed. Adapted from Mao et al[30].

4.2. **Polyelectrolyte Multilayer for Substrate Bonding**

As an alternative for avoiding the collapse or sag of nanochannels using bonding process at high temperature, silicon-to-glass bonding was here achieved by electrostatic interaction at lower temperature (180 °C) than conventional anodic bonding temperature (350 °C), and even at room temperature, as shown in Figure 4-3.

Poly(allylamine hydrochloride) (PAH) (Mw~70,000) / Poly(acrylic acid) (PAA) (Mw~90,000, 25% aqueous solution) multilayer thin films as a cationic and anionic polymers were assembled on glass or silicon substrates using a spinner at a fixed rotation rate (3,000 rpm) for 1 min. All the polymers were used after filtration with 0.2 μm pore-sized membrane. The deposition step were conducted as follows: PAH (pH 7.5), PAA (pH 3.5) and PSS (pH 4.7) solutions (10 mM with respect to the molecular weight of each repeat unit in 18 MΩ Milipore water) were prepared by adjusting the solutions pH by either HCl or NaOH. NaCl (100 mM) was added to the cationic PAH to adjust the solution ionic strength. The layer-by-layer deposition was carried out from

38

starting with the cationic PAH on glass substrates which were cleaned and dried by piranha and nitrogen gas for increasing the negative charge density on the surfaces. After the deposition of each polyelectrolyte layer on the surface, followed by thorough rinsing with Milipore water twice at the same spinning time and rate as the deposition process. After repeating the process until reaching 10.5, 20.5 or 25.5 layers for a top glass substrate and 10 layers for a bottom substrate with channels, the top and bottom substrates were assembled with the cationic PAH on the top and the anionic PAA on the bottom as the outermost layer as shown in Figure 4-3 (a).

Two substrates which have counter charged outermost layer were bonded through three different bonding methods, which are electrostatic interaction without heat, with heat and with chemicals as shown in Figure 4-3 (b), (c) and (d), respectively. The increase of overall bonding yield in (d) was caused by slow water evaporation kinetics at low temperature. To achieve the result in Figure 4-3 (d), 1-ethyl-3-(3-dimethyl aminopropyl) carbodiimide (EDC) (400 mM) and N-hydroxysuccinimide (NHS) (100 mM) were prepared in DI water as crosslinking agents between ammonium groups (-NH$_2$) of PAH and carboxlyate groups (-COOH) of PAA. The mixture(50:50 v/v) of the solutions was deposited on the bottom substrate with the anionic PAA as the outermost layer in the biohood. Top substrate with the cationic PAH as the outermost layer was placed on the bottom substrate and left bonded wafers for 6 hours in the biohood. The top and bottom substrates were crosslinked in aqueous EDC/NHS solution by a carbodiimide coupling reaction between the PAA and PAH chains. The covalent bonding made the PEM bonding robust and extremely difficult to wash off. The PEM layers were stable even when treated with methanol, 1 M HCl, and 1 M NaOH solutions for three days.

(A) glass

PAA pH=3.5

PAH pH=7.5

glass or silicon

➢ Experimental conditions

• PAH (pH=7.5), PAA (pH=3.5) and PSS (pH=4.7) were used

  - Method 1. Electrostatic interaction w/o thermal treatment

  - Method 2. Electrostatic interaction w/ thermal treatment at 180°C

  - Method 3. Chemically assisted by EDC-NHS at 25°C

➢ Chip scale bonding

(B) Method 1. (6hrs)

Bonded Area

$(PAH/PAA)_{10}, (PAH/PSS)_{20.5}$

(C) Method 2. (6hrs)

$(PAH/PAA)_{10}, (PAH/PSS)_{20.5}$

Method 2. (6hrs)

$(PAH/PAA)_{10}, (PAH/PSS)_{10.5}$

(D) Method 3. (6hrs)

$(PAH/PAA)_{10}, (PAH/PSS)_{25.5}$ w/ EDC-NHS

The role of EDC-NHS
Retarding water evaporation at low T increases bonding area

Figure 4-3 (a) The mechanism of electrostatic bonding by crosslinked PAH/PAA (b) bonding result without thermal treatment (c) with thermal treatment at 180 °C (d) with 1-ethyl-3-(3-dimethyl aminopropyl) carbodiimide (EDC) - N-hydroxysuccinimide (NHS), which is crosslinking agent and catalysts at room temperature, 25 °C.

Figure 4-4 shows that nanochannels were tightly sealed with a glass substrate by electrostatic bonding with the chemical crosslinking agents, EDC-NHS. Thus, this method can be applied to larger width planar channels without collapsing.

(a)

white line : walls
black line : nanochannels

(b)

white line : fluorescent dye in nanochannels
black line : walls
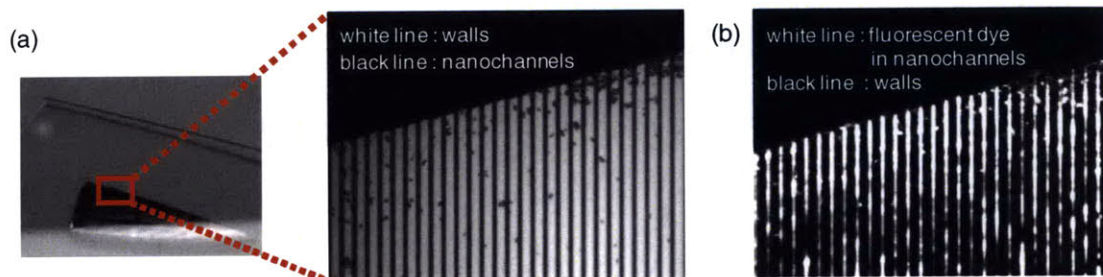
Figure 4-4 (a) The microscope images of bonded nanochannels under visible light and (b) nanochannels with fluorescent dye.

4.3. Conclusion

Since the main risk of micro-/nanochannel fabrication is the clogging or sagging of the apertures during high temperature bonding, anodic bonding (~350 °C) for silicon-glass and thermal fusion boding (~550 °C) for glass-glass, we have investigated the low temperature electrostatic bonding using polyelectrolyte multilayers (PEMs) in lieu of the conventional bonding methods. We have obtained clogging-free enclosed channels through electrostatic interaction of PEMs at 180 °C without cross-linking agents, EDC-NHS, and at 25 °C with EDC-NHS between silicon and glass substrates. The low-temperature bonding technique described here will provide an easy and alternative process for fabricating reliable micro- / nanofluidic devices uniform gap size along the channel. An important application of the devices is for medical or analytical use in contact with biological fluids. Therefore, the construction of protein- or cell-resistant surface is a crucial requirement. One strategy to reduce biofouling adsorption is surface modification by poly(ethylene glycol) (PEG) which has protein- and cell-repellent properties. Chapter 5 demonstrates the use of a novel polymer to prevent protein adhesion.

Chapter 5. Polyelectrolyte Multilayer for Surface Functionalization

5.1. Introduction

Silicon-based (e.g., silicon, glass, quartz, and PDMS) microfluidic devices have been extensively employed as an analytical tool or an medical microsystem[33]. However, these surfaces result in non-specific adsorption of reagent/sample molecules from the surrounding fluid (so called "biofouling"), which is often undesired for biological assays. When small sample quantities, such as rare proteins are involved, any loss of sample through the system may result in critical error in the final analysis[34]. In this chapter, we present a simple and widely applicable method to fabricate surface modified microchannels by cationic polymer, Poly(allylamine hydrochloride) (PAH), and non-biofouling materials such as polyethylene glycol (PEG).

5.2. Fabrication of PEG microchannels

Poly(dimethylsiloxane) (PDMS) is widely used to fabricate microfluidic channels because of its favorable mechanical and optical properties and its simple manufacturing by rapid prototyping. A microfluidic PDMS channel was fabricated by curing the prepolymer on silicon masters that had protruding features with the impression of microfluidic channels (100 μm in width, 10 μm in depth). To cure the PDMS prepolymer, a mixture of 10:1 silicon elastromer and the curing agent was poured onto the master and held at 70 °C for 2 hours. The PDMS mold was

then peeled from the silicon wafer. For bonding PDMS channels, a microfluidic mold and a glass slide were plasma cleaned for 40 s (PDC-32G, Harrick Scientific, Ossining, NY). After plasma treatment, the microfluidic mold was brought in contact with the substrate and firmly pressed to form an irreversible seal.

Then, polyelectrolytes were injected into the channel, which was cleaned and dried by nitrogen gas to increase the negative charge density on the entire surface. The layer-by-layer deposition was carried out by starting with the cationic PAH (pH=7.5) followed by the anionic PSS (pH=4.7), until reaching 5.5 layers with the outermost layer being PAH. After the deposition of each polyelectrolyte layer inside the surface, we applied thorough flushing with Milipore water.

Block copolymers[35] comprise two or more homopolymer subunits linked by covalent bonds. They have potential for a wide range of applications because of their unique properties that cannot be found in homopolymer or blend systems. Block copolymers consist of incompatible, chemically different homopolymers as blocks permanently connected to each other by unbreakable covalent bonds within one chain. Amphiphilic block copolymers are a type of block copolymer in which one block is hydrophilic and water-soluble, and the other block is hydrophobic, hence water-insoluble. Amphiphilic block copolymers[36] are a good example of A-B type diblock copolymers in which one block, A, is strongly attracted to a solid surface, and the other block, B, is repelled by the same solid surface when they are adsorbed from solution.

As a block copolymer, we used poly(ethylene oxide)-*block*-poly(methacrylic acid) (PEO-*b*-PMAA). A small amount (50 -200 µl) of PEG-*b*-PMAA (5 mM) injected into the positive charged channel. Poly(methacrylic acid) (PMAA) possesses pH-responsive properties, where the conformation and solubility of chain segments in aqueous media can be manipulated by pH[37-38].

43

The PMAA block forms negative charge in aqueous solution at pH > pK_a. The detailed acid-base chemistry is described in Appendix A. The PMAA block adheres onto a cationic PAH surface and forms the "anchor", whereas the repelled non-charged PEO block forms a polymer brush, the "buoy", that has a free end facing the solution as illustrated in Figure 5-1.

➢ Protein adsorption-resistant surfaces

PEO brush

• PAH-(PEO-b-PMAA) adsorption on substrate
  - Hydrophilic
  - Moves freely in aqueous solution
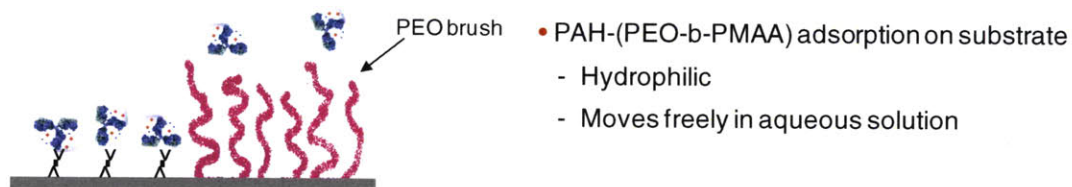
Figure 5-1 Schematic of asymmetric block copolymer chains adsorbed on the surface. The anchor block (PMAA) forms a discontinuous pancake patchwork in contact with the wall. The buoy chains (PEO) in pink are stretched in the solvent.

PEO adsorbed onto surfaces forms a highly hydrated layer that entropically and enthalpically prevents protein adsorption, bacterial adhesion and cellular adhesion due to its strong affinity for water molecules.

5.3. Non-specific protein adsorption on PEM-coated channels

To assess the non-biofouling nature of PEG microchannel, the fluorescein-labelled Lectin was flowed through the channels (PEO treated and PEO untreated). The isoelectric point (pI), the pH at which a particular molecule or surface carries no net electrical charge, for Lectin is around 4.7. Since the net charge on the molecule is affected by pH of their surrounding environment and can become more positively or negatively charged due to the loss or gain of protons (H^+), Lectin

forms positive charge dissolved in acetate buffer (pH = 5) at the pH conditions above the pI value of itself, 4.7. To test for adhesion of Lectin within microfluidic channels, the biomolecues were pumped through the microchannels for 30 min at a flow rate of 5 μL min^{-1}. Then, the channels were rinsed thoroughly with DI water and subsequently analyzed using an inverted fluorescent microscope (IX71, Olympus).

The results show that the PEO treated surface reduces the intensity near the wall surface as shown in Figure 5-2. This quantitative analysis indicates that the PEO coated channel was resistant against protein adhesion. In comparison to controls (PEO untreated channel), the relative adsorptions were less than 38% (before DI flushing) and 27% (after DI flushing).
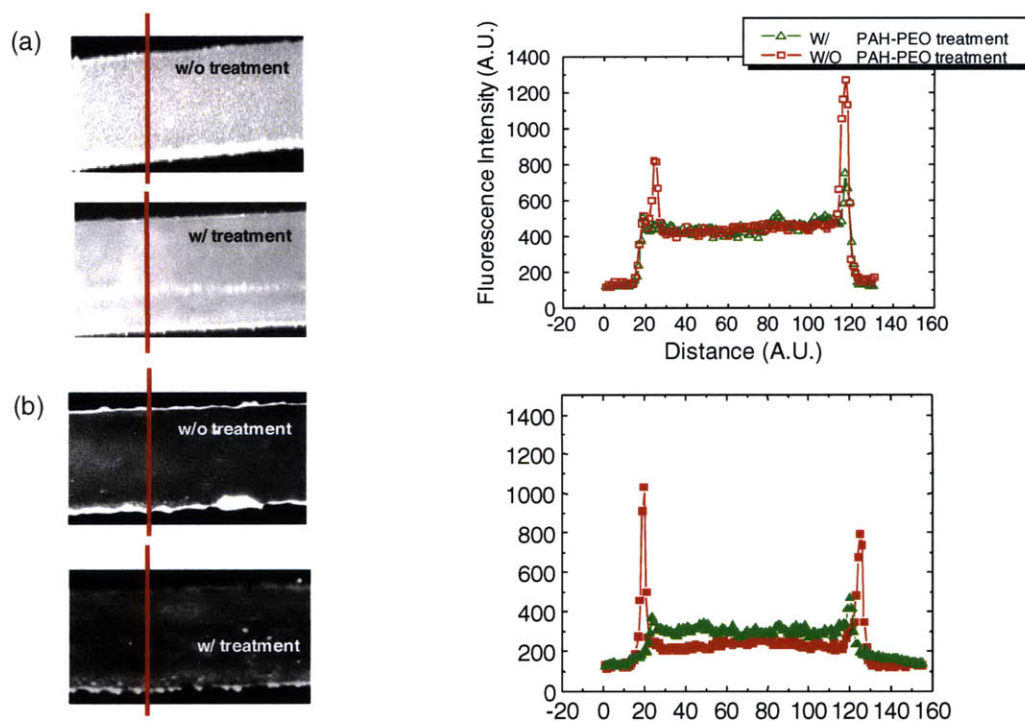
Figure 5-2 Microchannel (depth 10 μm) filled with Lectine in acetate buffer pH5 (+) (a) before and (b) after DI flushing.

45

5.4. Conclusion

We have incorporated PEO into polyelectrolyte multilayers by attaching PEO to the backbone of poly(methacrylic acid) (PMAA), a negatively charged biopolymer. Polyelectrolyte multilayers topped with a PEO-*b*-PMAA block copolymer significantly reduced protein attachment of Lectin. It can be an effective way of controlling cellular and bacterial adhesion by enhanced resistance to proteins. Compared to the standard chemical grafting techniques used for PEO surface functionalization, multilayer film depositing has the advantage of being rather independent of the nature or topology of the material. Thus, PEM films have been constructed using PEO-grafted polymers or by depositing a PEO layer on top of the films, yielding a non-fouling multilayer film. These PEO coated channels are advantageous in that they use very small volumes of samples / reagents and can be potentially scaled up for high throughput analysis. However, controlling topographical features and spatial presentation of surface molecules is important for the development of cell and protein arrays for drug discovery, diagnostic assays and biosensors. To obtain features with controlled topographical features, technique providing control over both surface topography and spatial presentation of surface molecules over a variety of feature sizes are discussed in Chapter 6.

Chapter 6. Fabrication of selective anti-biofouling surfaces

6.1. Introduction

There has been great interest in micro- and nanopatterning to create functional biomolecular arrays for *in vitro* diagnostics, biosensors, biochips, biomedical microdevices, and tissue engineering[39-40]. Cell patterning, the method of cell immobilization on a desired area, is an especially important tool for investigating the interactions of cell-surface, cell-cell, cell-antibiotics, and cell-biomolecules[41-42]. In nature, microbial communities inhabit matrices with intricate spatial structure[43-44]. Many species of bacteria coexist as microcolonies separated by a few hundred micrometer[45-46]. This spatial structure has been hypothesized to be important in microbial ecology[47-50]. However, on this small scale spatial structure is difficult to control in natural environments. Furthermore, microscale spatial structure has not been controlled and varied experimentally to understand its effect on the stability of bacterial communities. To address these limitations, we have developed a technique for fabricating bacterial micropatterning by constructing a synthetic community of *P.aeruginosa* PA01, an opportunistic pathogen in humans and a model organism widely used for biofilm studies.

Many approaches to protein patterning have been reported, including dip-pen lithography[51], inject printing[52], photolithography[53], microcontact printing (μCP)[54], and spotting[55-56]. Although spotting, photolithography, and inject printing easily create micropatterns of cells and dip-pen lithography shows itself to be suitable for fabricating nanopatterns, these methods depend heavily on available facilities. Thus μCP has been introduced as an alternative method, being simple, flexible, and well adapted for research laboratories not equipped with photolithographic

tools and clean room facilities. The successful application of μCP of biomolecules from a microstamp onto a surface, however, is dependent upon the time required to progress from drying the stamp to printing proteins as well as upon the property of immobilizing surfaces[57]. In addition, although μCP is a relatively simple and versatile technique of cell patterning, the non-patterned regions (background) must be modified with biological barriers to prevent nonspecific adsorption of cells after the process of printing of proteins onto the desired surface has been completed. Therefore, one must develop a novel patterning method to create a functional surface to capture and localize cells within particular regions combining with the background regions where reduce nonspecific adsorption of cells. An efficient cell patterning for flexibility in size as well as in the shape of the patterns could be of benefit.

To prepare the functional surface with the desired property of protein patterning, conventional methods of surface modification have been performed using delicate multistep[58-61]. However, a few of the available methods of chemical modification might limit the control of surface property on the desired area because the modification area is difficult to control spatially[58-59,61].

Here we present an alternative approach, both simple and reliable, for the preparation of functionalized surfaces using a soft-lithographic technique as well as poly(ethylene glycol)-poly(lactide) diblock copolymer (PEG-PLA) as a novel polymer to prevent nonspecific binding of cells. This method combines an efficient surface modification using polymeric thin film of self-assembled polyelectrolyte multilayers (PEM) with micromolding in capillaries (MIMIC) of PEG-PLA. First, the surface is modified with a self-assembled multilayer of PEM using a layer-by-layer (LbL) technique (section 6.2). The passivation of the background with PEG-PLA can be obtained using the MIMIC method (section 6.2). The functionalized surface can be easily applied

to micropatterns of cells on the desired area. The PEG-PLA coating on the background has served as a biological barrier against the nonspecific adsorption of proteins because of the resistant nature of PEG. In contrast to the widely used μCP, it simultaneously provides both a selective cell binding region (the exposed PEM region) and a biological barrier (the anti-biofouling region involving PEG-PLA).

Our technique rests on a simple process to create the functionalized surface for efficient micro patterning of cells in various sizes and shapes as well as using a variety of material and substrates. It can be fabricated by the use of micromolding in capillaries (MIMIC) of poly(ethylene glycol)-poly(lactide) diblock copolymer (PEG-PLA) and self-assembled polyemetrolyte multilayers (PEM). Compared to other self-assembly techniques such as self-assembled monolayers (SAMs) or Langmuir-Blodgett (LB) films, an LbL assembly is far more versatile[62-64]. Also, a variety of materials, including proteins, DNA, dyes, polymers, and inorganic materials, can be incorporated into the films. In addition, a wide range of substrates can be employed; these substrates include glass, silicon, silicon dioxide, metal, and polymers. However, depending on the technique utilized, the choice of a specific surface might be limited due to the interaction with the deposited molecules. For example, molecules containing a thiol group always require a gold surface for deposition. In contrast, the MIMIC combined with an LbL coating provides a general platform for biomolecular patterning compatible with a broad range of materials.

6.2. Experiments

PEM Coating on Glass

A glass slide was cleaned using a piranha solution consisting of a 4:1 mixture of 50% aqueous solution of H_2SO_4 and 30% aqueous solution of H_2O_2, rinsed sequentially with deionized water, ethanol, and acetone, and finally dried with nitrogen. The activated glass was spin-coated with polyallylamine hydrochloride (PAH) at 4000 rpm for 15 s. To remove the unbound PAH, the substrate was washed with distilled water for three times and then spin-coated with a solution of polystyrene sulfonate (PSS) (20 mM; pH 9.0) at 4000 rpm for 15 s (Figure 6-1 a).
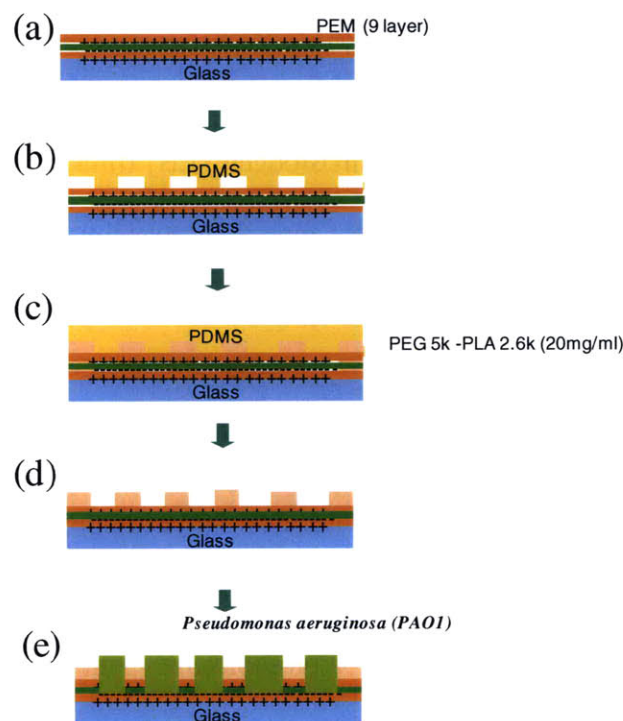
Figure 6-1 Schematic diagram of protein patterning on a functionalized surface prepared with PEM coating and MIMIC of PEG-PLA. (a) substrate coating with PEM (PAH/PSS) (b) placement of PDMS micromold onto the PEM surface by conformal contact (c) MIMIC of PEG-PLA polymer by capillary action (d) removing the PDMS micromold (e) loading of proteins onto the fabricated surface.

This procedure was repeated until the desired number of polyelectrolyte layers was assembled with a positively charged PAH as the outermost layer, because negatively charged proteins bind well on positively charged polymeric surfaces owing to the strong electrostatic interaction force.

The preparation of functional surfaces using the MIMIC method

PDMS (Sylgard 184, Dow Corning, USA) molds having micro- or nano-structures were fabricated against a complementary relief structure that was prepared using conventional photolithography. Each PDMS mold was cut so that it formed a network with open ends. The trimmed PDMS mold was placed on PEM-coated glass to achieve conformal contact (Figure 6-1b). When poly(ethylene glycol)–poly(D,L-lactide) diblock copolymer (PEG5k–PLA2.6k; 20mg ml^{-1}) was placed at the open ends of the molds, the PEG-PLA spontaneously filled the empty spaces through capillary action (Figure 6-1 c). PEG–PLA was bound with polyelectrolyte multilayers for 1 h and then the PDMS micromold was peeled off (Figure 6-1d).

6.3. Results and Discussion

Preparation and characterization of the functional surface

To confirm the selective binding of PEG–PLA onto PAH as a top layer of PEM, contact angle analysis was performed after the deposition of PEG–PLA over positively charged (PAH) surfaces as shown in Figure 6-2. As a control experiment, the PEM surface was also examined. The average contact angle of PEM surface having a PAH top-layer was about 51°. The PEG-PLA deposited onto the PAH surface showed a decrease in contact angle (25°) compared to the

51

contact angle for the PAH top-layer case. It indicated the successful coating of PEG–PLA onto the PAH polymeric layer. The decrease of the water contact angle suggests that the buoy chains (PEG) are exposed in the water, whereas the anchor block (PLA) is strongly bound onto the PEM surface layer as shown in Figure 5-1.

Because ethylene oxide groups in PEG-PLA are hydrophilic, we can imagine that the PEG portion is exposed and not buried in the PEM surface; although the precise nature of this arrangement has not been firmly established, the PEG chains form a brush-like structure, and the PEG-PLA deposited surface results in the decrease of the water contact angle.
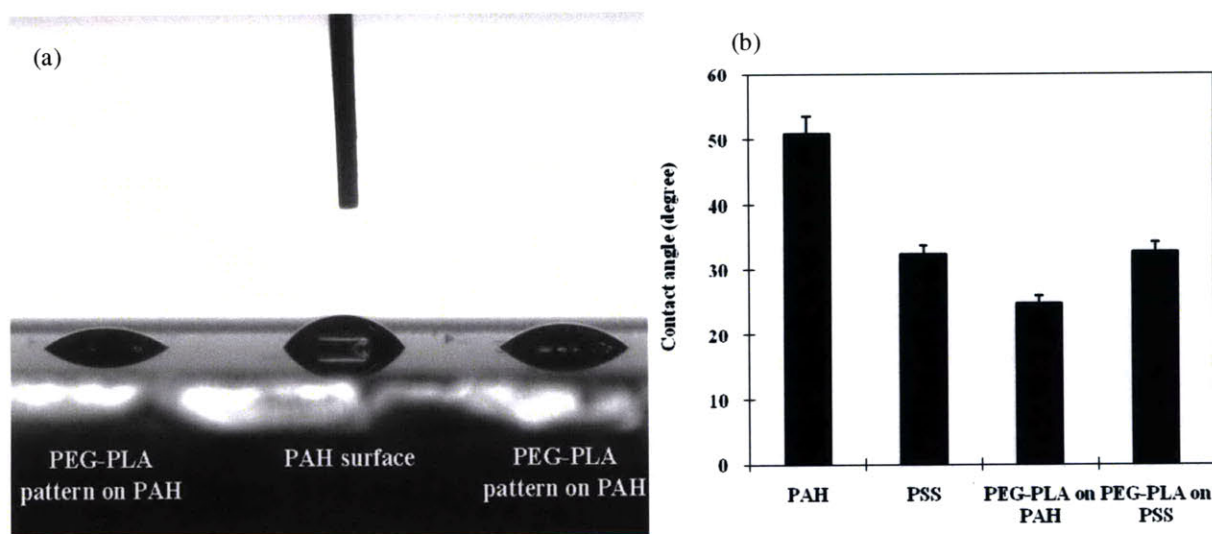
Figure 6-2 (a) image of water contact angles onto a PEG-PLA coated surface and sole PEM surface having PAH as a top layer; the contact angles are 25° and 51°, respectively. (b) the change of water contact angles.

We also characterized the topology of the functionalized surface using atomic force microscopy (AFM). When compared to each other, these images indicate that the topological changes of the surface are attributable to the selective deposition of PEG-PLA onto the PEM surface through the MIMIC process. Figure 6-3 shows the topographic changes of PEM and PEG-PLA treated surfaces before and after the washing process. The flatness of PEM coated surface confirms that LbL process has been correctly performed and is stable for the preparation of a homogeneous thin film. After the deposition of PEG-PLA onto PEM using the MIMIC process, the topographic contrast between PEG-PLA and PEM region is clearly shown and the height of the edge region of the pattern is attributable to the increase in the amount of PEG-PLA along the edge of the micromold because of capillary wetting of the PEG-PLA polymer during the MIMIC process. During the final washing, the roughness is dramatically reduced from 114 nm to 23 nm due to the successful removal of PEG-PLA, which is only weakly bound to the PEM surface. The measured height of deposited PEG-PLA (23 nm) confirms that the orientation of the binding PEG-PLA polymer onto PEM is upward PEG, because the exposed length of PEG5k chain is precisely matched with a recently reported value[65]. The clear AFM image of a sharp-line edge between the PEM and PEG-PLA region suggests the occurrence of a laterally homogeneous and well-defined surface modification. The results hint at the possibility of fabrication of smaller feature sizes with appropriate molds having small features as well as mechanical properties resistant to the collapse of micro- or nanostructures.
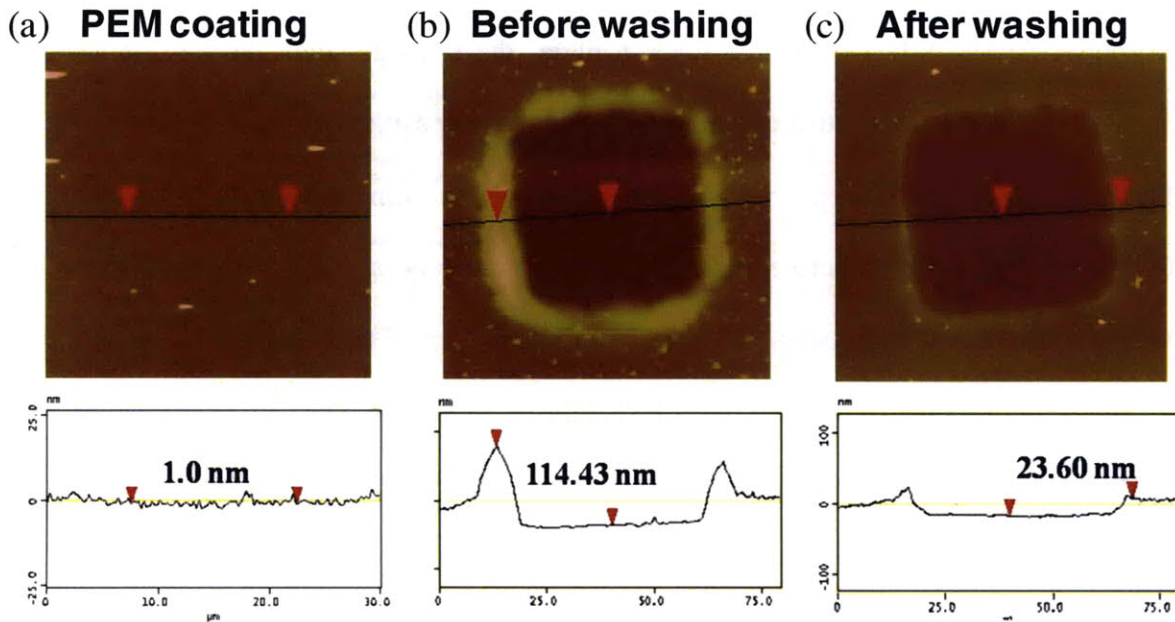
Figure 6-3 The characterization of the fabricated surface using AFM. (a) topological analysis of homogeneously coated surface with PEM (b) the functionalized surface containing PEG-PLA and PEM region using the MIMIC process before the washing step and (c) after the washing step; the scanning area is ~ 30 × 30 μm.

Micro/nanopatterning of bacteria onto a functionalized surface

To investigate the feasibility of bacterial micropatterning, we tested it with the bacteria *Pseudomonas aeruginosa* PA01, an opportunistic pathogen in humans and a model organism widely used for biofilm studies. As is shown in Figure 6-4, the images of micropatterns display bacterial patterns reflecting the surface patterning. Larger bacterial densities observed in the exposed PEM region indicate that the preparation of a functional surface was successful The dramatically decreased bacterial density on the PEG-PLA region shows the reduced nonspecific binding of the bacteria onto the background. When PEG-PLA is grafted to the surface, a close association between water molecules and PEG exists due to hydrogen bonding. The formation of

a hydration layer hinders the nonspecific adsorption of bacteria[66-68]. The experimental results mentioned above confirm that the PEG-PLA diblock copolymer as a biological barrier is successfully deposited onto the desired background region and that we can freely control the size and shape of micropatterns of bacteria. The micropatterning of bacteria clearly demonstrates that it is possible to fabricate uniform bacteria microarrays on the functionalized surface using MIMIC of PEG-PLA and a multilayered coating of PEM.
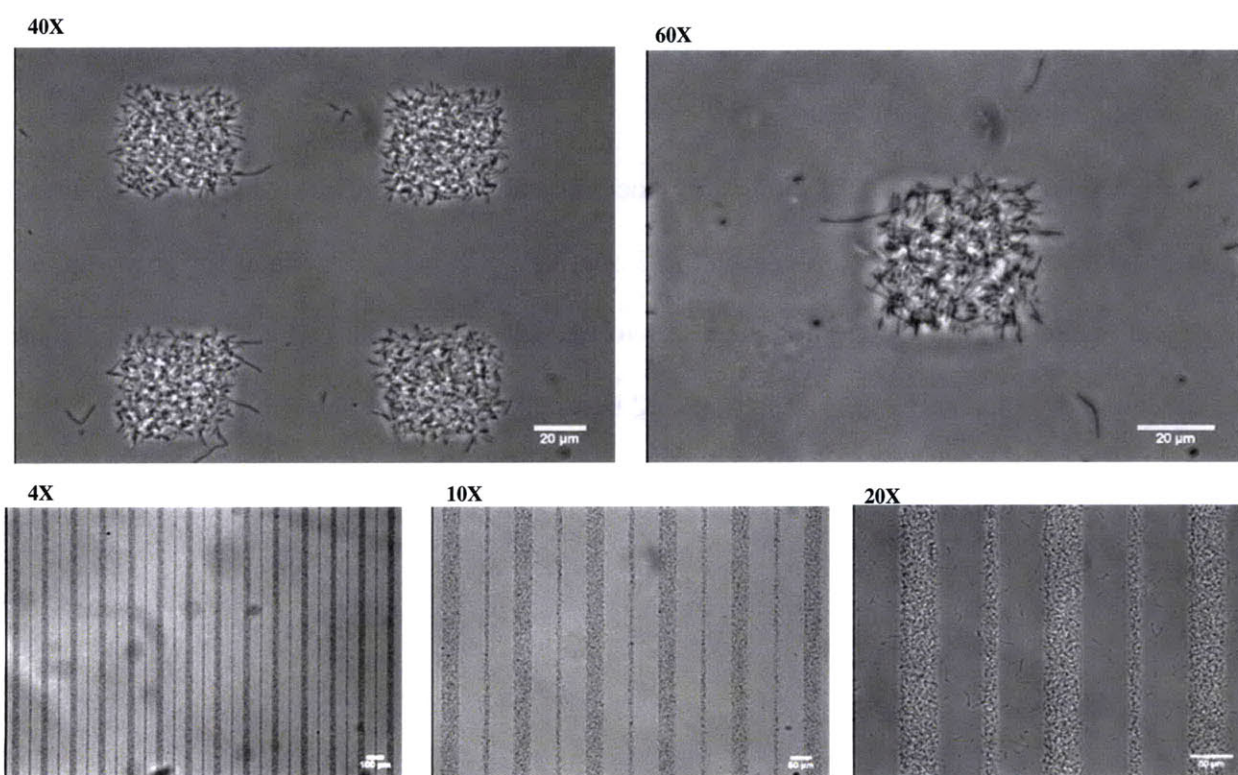
Figure 6-4 Selective attachment of bacteria to chemically micropatterned channels. A suspension of the bacteria *P. aeruginosa* PA01 was left in contact with the micropatterned surface for 10 minutes. This resulted in attachment to the PEM coated regions. In the top two panels, the PEM coated regions had a 50x50 μm square shape. A small number of squares is shown, out of the many hundreds of identical squares in the microchannel. The lower three panels show bacteria attached to an array of PEM stripes (20 and 50 μm wide).

6.4. Conclusion

We have proposed a simple and reliable bacterial patterning method combining MIMIC with self-assembled PEM multilayers. We have also demonstrated a technique involving bacterial patterning at the microscale. The use of PEG-PLA to prevent the nonspecific binding of bacteria enables the high-resolution patterning of bacteria onto the desired area with flexibility in pattern, size and shape. This approach requires no hazardous photolithography steps, use of toxic solvents, or expensive equipment.

This method will be useful in integrating bacteria and micropatterns to study biofilm formation. It provides a simple, user-configurable, and relatively inexpensive method for growing biofilms in both static and flow conditions in order to understand the role of biofilm size and shape on disruption by shear, diffusion-limitation, and hydrodynamic niche selection by bacteria.

Chapter 7. Summary and Outlook

7.1. Summary

The overall goal of this thesis was to exploit the versatility of the polyelectrolyte multilayer (PEM) to fabricate a novel micro/nanofluidic device for high-throughput applications and develop a new platform for creating parallel, reproducible bacterial patterning for studying the chemical, physical, and environmental factors that govern biofilm development. Since polyelectrolyte multilayers (PEMs) offer a simple, water-based, versatile platform for exploring biomaterials with cell and bacterial control functionalities, it can incorporate micro- and nanofabrication technology.

BioMEMS approaches have not yet been widely used in the biological and clinical communities since they have lower sample throughput and until recently were quite limited compared to traditional membrane materials such as gel in the smallest size that was achievable. To widely use such devices, the fabrication process of micro/nanofluidic devices must be addressed. Therefore, a first major thrust area of this research was the development of micro/nanofluidic devices for high-throughput with near-molecular dimensions. We have developed novel strategies for fabricating massively-parallel, high-aspect-ratio vertical nanochannels by a combination of anisotropic etching and thermal oxidation. To reduce the gap of the nanochannels down to 50 nm, polyelectrolyte multilayers (PEMs) were employed because the layers can be controlled on the nanometer scale, providing precise control over layer thickness.

The other challenge in making BioMEMS devices widely applicable is to replace conventional bonding methods such as anodic bonding and thermal fusion bonding. Since these bonding

57

technique are usually performed at very high temperatures (350 °C for anodic bonding and 550 °C for thermal fusing bonding), micro- and nano structures can be easily distorted and bended, resulting in unreliable bioanalysis systems. Therefore, we investigated low-temperature bonding method using PEMs, because surface charge and surface roughness can be precisely controlled depending on pH condition and ionic strength of the polyelectrolyte solutions during the dipping process. We have demonstrated successful bonding through electrostatic interaction of PEMs at 180 °C without cross-linking agents, EDC-NHS, and at 25 °C with EDC-NHS between silicon and glass substrates.

A further challenge in the use of micro-/ nanofluidic devices for improved bioanalytical and diagnostic devices is the non-specific adsorption of reagent/sample molecules. Hence, there is considerable interest in the development of non- or low-fouling surfaces. We fabricated polylelectrolyte multilayers topped with a PEO-b-PMAA block copolymer. PEMs were deposited to increase the amount of loading of PEO-b-PMAA block copolymer as well as to be independent of the nature or topology of substrates. The experimental results showed a dramatic decrease of non-specific adsorption of Lectin on PEO treated channels (38% before DI flushing and 27% after DI flushing) in comparison to controls (PEO untreated channel). This can be an effective way of controlling cellular and bacterial adhesion by enhanced resistance to proteins.

As stated above, one potential method to switch surface properties that could potentially be useful for patterning cells is the use of layer-by-layer assembly of polyelectrolytes. In the second part of the thesis, we have explored the possibility of patterning bacteria by the use of micromolding in capillaries (MIMIC) of poly(ethylene glycol)-poly(lactide) diblock copolymer (PEG-PLA) onto polyelectrolyte multilayers (PEMs). The patterned surface therefore consists of

two sets of regions: PEMs and PEG-PLA. The first (PEMs) promotes adhesion of cells, whereas the latter (PEG-PLA) hinders adhesion by preventing nonspecific binding. To test this method we used *P. aeruginosa* PAO1 bacteria, depositing a drop on the micropatterned surface. The coated surfaces by PEMs, which are relatively hydrophobic (contact angle, 51 °C) compared to PEG-PLA coated regions (contact angle 25 °C), showed excellent results for the micropatterning of bacteria. These devices will be ideal to acquire a deeper understanding of bacteria-surface interactions and the effect of biofilm size on subsequent biofilm dynamics, including susceptibility to disruption by shear and the ability of a biofilm patch of a given size to harbor multiple bacterial strains.

7.2. **Outlook**

Nanochannels on a chip have the potential to be used for biotechnological applications such as immunoassay, proteomics, or DNA molecule separation. These solid-state nanochannels are much more robust than polymer membranes, both chemically and mechanically. Gap sizes can be well controlled by polyelectrolyte multilayers (PEMs) deposition. The uniformity of the nanochannels allows stable operation and repeatability. It is expected that these nanochannels could be essential in the development of bioanalysis system. In addition, the micropattern arrays created using micromolding in capillaries (MIMIC) of poly(ethylene glycol)-poly(lactide) diblock copolymer (PEG-PLA) onto polyelectrolyte multilayers (PEMs) make it possible to fabricate different shapes and dimensions to control the spatial adhesion and growth of cells on surfaces. These techniques have the potential to help shed shed light on the relationship

between the size of biofilm microcolonies on disruption by shear, diffusion-limitation, and hydrodynamic niche selection by bacteria.

For commercial application, further research is clearly necessary. To use nanofluidic channels for separation and manipulation of a wide spectrum of biomolecules including proteins, organelles, and carbohydrates based on size and electrostatic interaction by changing the surface charge density, additional experiments need to be carried out to determine the ultimate minimum gap size that can be uniformly attained using polyelectrolyte multilayers (PEMs) deposition. The work presented here represents a first step in this direction.

APPENDIX A

A.1. Review of Acid-Base Chemistry : Controlling the Degree of Ionization[69]

1. Definitions:

Bronstead and Lowry : acid is a substance that can donate protons; bases accept protons

Lewis : acid is an electron pair acceptor; base is an electron pair donator

       (more general definition)

2. Acid-Base reaction:

An acid-base reaction in equilibrium can be written as follows:

$$\underset{\text{acid}}{HA} + \underset{\text{base}}{H_2O} \leftrightarrow \underset{\substack{\text{Conjugate}\\\text{acid}}}{H_3O^+} + \underset{\substack{\text{Conjugate}\\\text{base}}}{A^-}$$
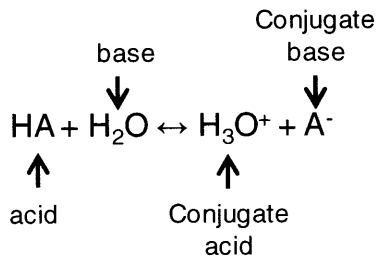
For a given set of reaction conditions, e.g. temperature and pressure, the ratio of reactants and products reach a constant value at equilibrium. From the equilibrium reaction, we can define an equilibrium rate constant, k,

$$k = \frac{[H_3O^+][A^-]}{[HA][H_2O]} \tag{A.1}$$

For weak acid, $k < 1$,

In dilute aqueous solutions, $[H_2O]$ is constant. Therefore, we can define another dissociation rate constant, k_A, for acids in aqueous solutions.

$$k_A = \frac{[H_3O^+][A^-]}{[HA]} \tag{A.2}$$

The expression for k_A can be further simplified for the case of water because $[H_2O]$ is constant:

$$k_w = [H_3O^+][OH^-] = 10^{-14}M^2 \tag{A.3}$$

In pure water $[H_3O^+$ or $H^+] = [OH^-] = 10^{-7}$ M at 25 °C

Because the concentrations of the acidic and basic species can vary by orders of magnitude, it is more convenient to refer to concentrations using logarithmic scale: $pH = -log[H^+]$

3. Henderson-Hasselbach Equation:

From the expression of k_A above, we can write an equation that relates pk_A of a species to the pH of its solution. This is known as the Henderson-Hasselbach Equation:

$$pH = pK_A + log\frac{[A^-]}{[HA]} \tag{A.4}$$

A few useful rules of thumb can be interpreted from the Henderson-Hasselbach Equation.

1. pk_A of an acid is equivalent to the pH of solution when molar concentrations of acid and conjugate base are equal (midpoint). i.e., the pH value at which an acid is half-ionized.

2. If pH of solution = pk_A + 1, then 90% of the species is deprotonated, i.e., more [A⁻] than [HA]

3. If pH of solution = pk_A - 1, then 90% of the species is protonated. i.e. more [HA] than [A⁻]

4. All of the species is deportonated or protonated if pH is +/- 2 of its pk_A.

5. When an acid becomes deprotonated, it becomes ionized while when a base becomes protonated it becomes ionized.
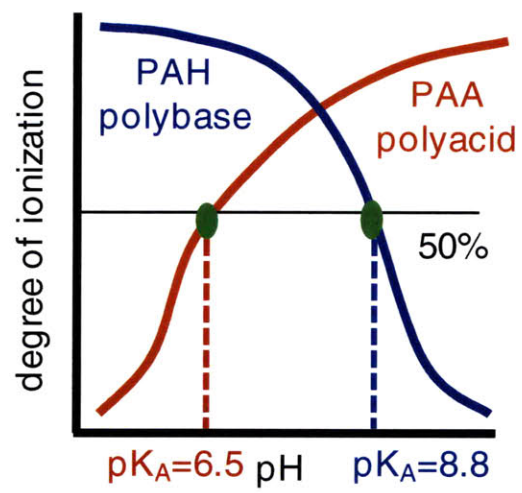
Figure A-1 Titration curve of weak polyelectrolytes

APPENDIX B

B.1. Process Flow of Nanochannel Fabrication on Silicon

(a) Photolithography for nanochannel (I-stepper)

↓ 40 nm ↑

(b) Si etching using RIE etcher (40nm)

(c) Photolithography for microchannel (I-stepper)

↓ 40 nm ↑   ↕ 2 um

(e) Si Etching using RIE etcher (2um)

(f) SiNx deposition (5000A) for KOH mask

(g) Photolithography for SiNx etching

(h) SiNx etching (5000A) using RIE for reservoir patterning

(i) Si Etching-through for reservoir formation

(j) SiNx etching using HF solution

(k) Thermal oxidation (4000A) for anodic bonding

Glass

(l) Anodic bonding

Figure B-1 Standard process flow of nanochannel fabrication on silicon

B.2. Process Flow of Nanochannel Fabrication on Glass

5" Pyrex wafers, red process

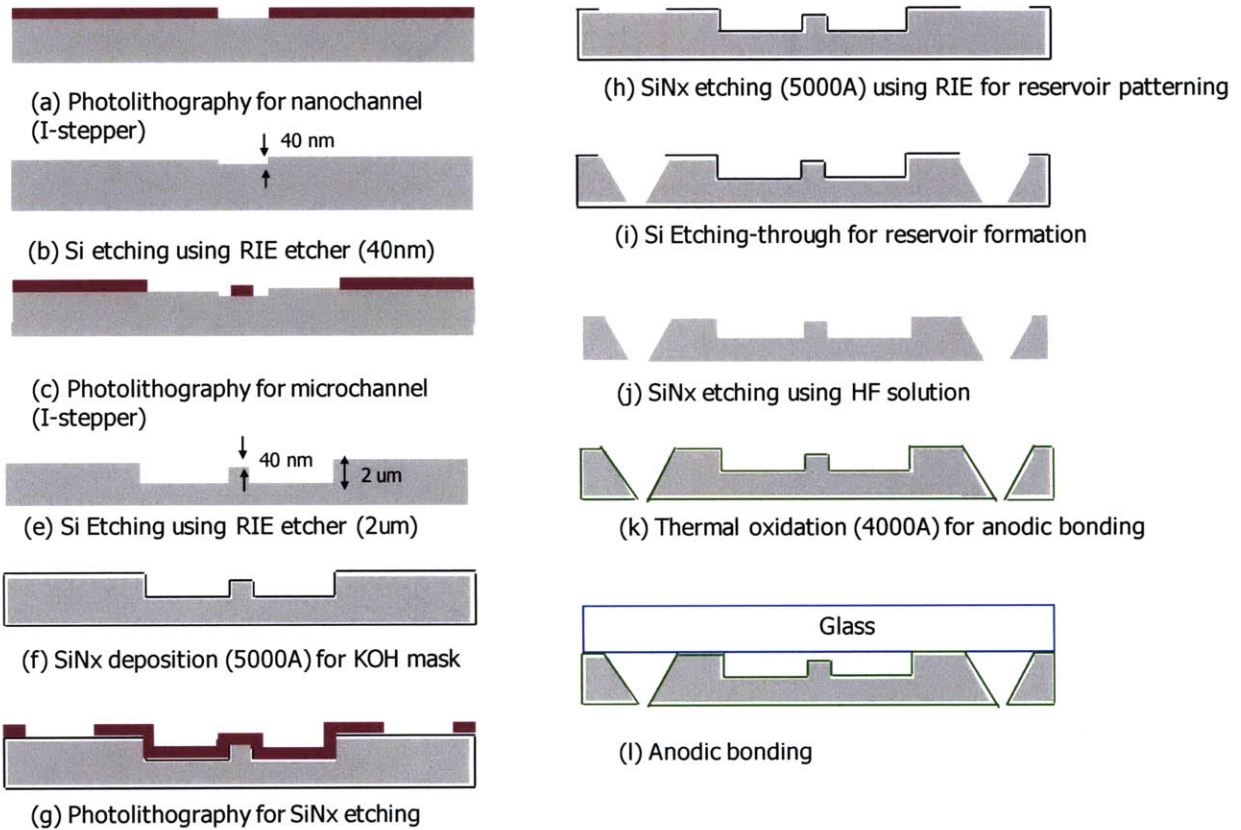| Step	Action	Machine
	Pattern nanochannels	
1_1	Piranha cleaning	Acid-hood_TRL_red
1_2	HMDS coating	HMDS_TRL_red
1_3	Resist coating(ImageReverse PR)	Coater_TRL_red
1_4	Prebake(30mins, 90C)	Prebakeoven_TRL
1_5	Exposure(3.5s)	EV1_TRL_red
1_6	Postbake(30mins, 90C)	Postbakeoven_TRL
1_7	Flooding(60sec)	EV1_TRL_red
1_8	Development(90sec or until clear)	Photo-wet_TRL_Au
1_9	Descuming(5min, 1000W)	Asher_TRL
1_10	Wet etching, BOE(1min30sec, ~40~45nm)	Acid-hood_TRL_red
1_11	Resist removal, Piranha	Acid-hood_TRL_red
	Pattern microchannels	
2_1	Piranha cleaning	Acid-hood_TRL_red
2_2	dehydration(60mins)	UV-ozone_TRL_red
2_3	Metal Mask(20nm Cr, 100nm Au) deposition	ebeamAu
2_4	HMDS coating	HMDS_TRL_red
2_5	Resist coating(Standard PR)	Coater_TRL_red
2_6	Prebake(30mins, 90C)	Prebakeoven_TRL
2_7	Exposure(3sec)	EV1_TRL_red
2_8	Development(~75sec or until clear)	Photo-wet_TRL_Au
2_9	Postbake(30mins, 120C)	Postbakeoven_TRL
2_10	Au Etching, Aqua Regia or Au etchant(30sec)	Acid-hood_TRL_red
2_11	Cr Etching, CR-7(25sec)	Acid-hood_TRL_red
2_12	Pyrex Etching(650:200:150, H2O:HF:HNO3),08um/min	Acid-hood_TRL_red
2_13	Solvent Cleaning(Acetone,Methanol,DI water)	Photo-wet_TRL_Au
2_14	Au Striping, Aqua Regia or Au etchant(2mins or until clear)	Acid-hood_TRL_red
2_15	Cr Striping, CR-7(2mins or until clear)	Acid-hood_TRL_red
2_16	Resist removal, Piranha	Acid-hood_TRL_red
	Pattern access holes / Bonding	
3_1	Drilling holes on glass (by SensorPrep)	Resonetics-Laser_EML
3_2	Surface cleaning, Piranha	Acid-hood_TRL_red
3_3	Surface activation, ammonium hydroxide(30min)	Acid-hood_TRL_red
3_4	Glass-glass bonding(550C, overnight)	Box-Furnace_EML

Table B-1 Process flow of nanochannel fabrication on glass

B.3. Process Flow of Microchannel Fabrication on PDMS

(A)

(a) Bare silicon wafer   (b) Photoresist(SU8) coating   (c) Photolithography   (d) SU8 master on silicon

(B)

(a) PDMS pouring / curing   (b) Peeling off from the Si master   (c) Punching holes   (d) PDMS mold for chemical pattering (1) / main channel (2)

(C)

(a) Bare glass slide   (b) Bonding with PDMS for patterning   (c) Injecting Teflon or OTS   (d) Detaching PDMS   (e) Bonding with PDMS channel
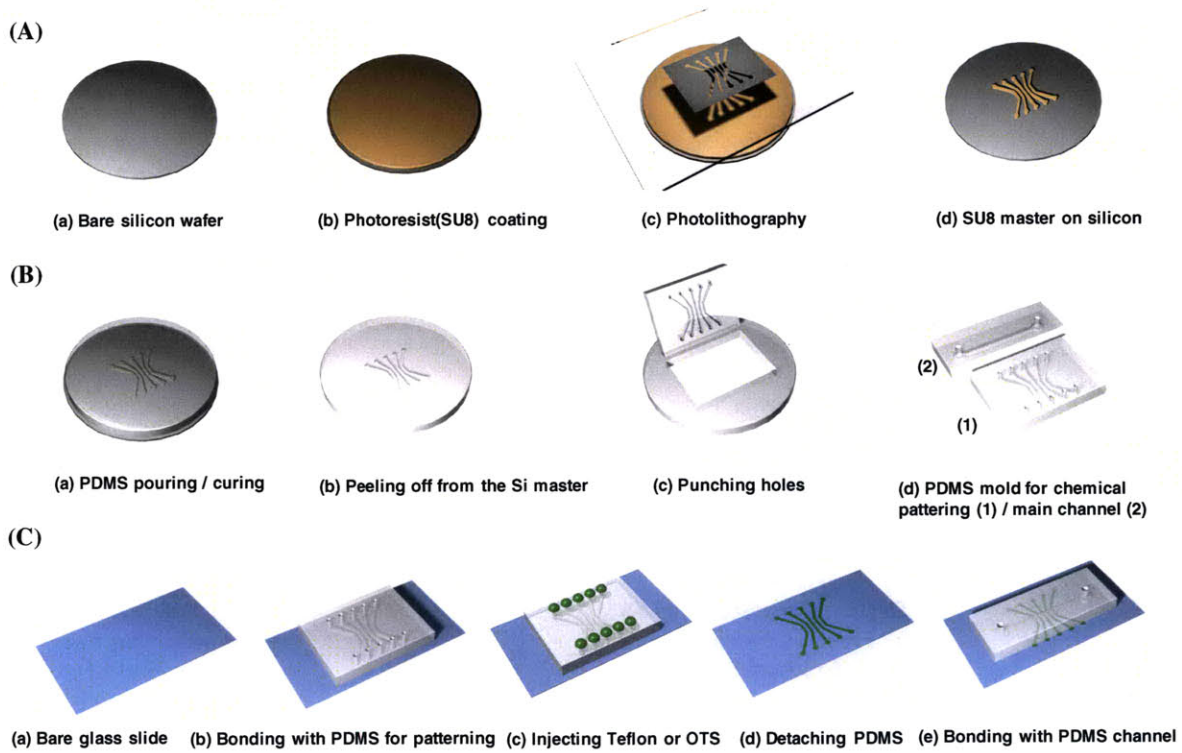
Figure B-2 Standard process flow of chemically patterned microfluidic channels on PDMS (A) Master fabrication with SU8 (B) PDMS fabrication for chemical patterning (1) / main channel (2) (C) PDMS bonding with chemically patterned glass slide

Bibliography

1. Tegenfeldt, J.O., *et al.* Micro- and nanofluidics for DNA analysis. *Anal Bioanal Chem* **378**, 1678-1692 (2004).

2. Delft, K.M.v., *et al.* Micromachined Fabry-Pérot Interferometer with Embedded Nanochannels for Nanoscale Fluid Dynamics. *Nano Lett.* **ASAP Web Release**(2006).

3. Mao, P. & Han, J. Fabrication and Characterization of 20 nm Nanofluidic Channels by Glass-Glass and Glass-Silicon Bonding. *Lab Chip* **5** 837 - 844 (2005).

4. Han, J. & Craighead, H.G. Separation of Long DNA Molecules in a Microfabricated Entropic Trap Array. *Science* **288**, 1026-1029 (2000).

5. Fu, J., Schoch, R.R., Stevens, A.L., Tannenbaum, S.R. & Han, J. Patterned anisotropic nanofluidic sieving structure for continuous-flow separation of DNA and protein. *Nature Nanotechnology* **accepted for publication**(2007).

6. Wang, Y.-C., Stevens, A.L. & Han, J. Million-fold Preconcentration of Proteins and Peptides by Nanofluidic Filter. *Anal. Chem.* **77**, 4293-4299 (2005).

7. Huang, L.R., *et al.* A DNA prism for high-speed continuous fractionation of large DNA molecules. *Nat. Biotechnol.* **20**, 1048-1051 (2002).

8. Saleh, O.A. & Sohn, L.L. An Artificial Nanopore for Molecular Sensing. *Nano Lett.* **3**, 37-38 (2003).

9. Karnik, R., Castelino, K., Fan, R., Yang, P. & Majumdar, A. Effects of biological reactions and modifications on conductance of nanofluidic channels *Nano Lett.* **5**, 1638-1642 (2005).

10. Fu, J., Schoch, R.R., Stevens, A.L., Tannenbaum, S.R. & Han, J. Patterned anisotropic nanofluidic sieving structure for continuous-flow separation of DNA and protein. *Nature Nanotechnology* **2** 121 - 128 (2006).

11. Wang, Y., Stevens, A. & Han, J. Million-fold preconcentration of proteins and peptides by nanofluidic filter. *Anal. Chem* **77**, 4293-4299 (2005).

12. Decher, G., Hong, J. & Schmitt, J. Buildup of ultrathin multilayer films by a self-assembly process. III: Consecutively alternating adsorption of anionic and cationic polyelectrolytes on charged surfaces. *Thin solid films* **210**, 831-835 (1992).

13. Lvov, Y., Decher, G. & Sukhorukov, G. Assembly of thin films by means of successive deposition of alternate layers of DNA and poly (allylamine). *Macromolecules* **26**, 5396-5399 (1993).

14. Lvov, Y., Haas, H., Decher, G., Moehwald, H. & Kalachev, A. Assembly of polyelectrolyte molecular films onto plasma-treated glass. *The Journal of Physical Chemistry* **97**, 12835-12841 (1993).

15. Decher, G., Lvov, Y. & Schmitt, J. Proof of multilayer structural organization in self-assembled polycation-polyanion molecular films. *Thin solid films* **244**, 772-777 (1994).

16. Bertrand, P., Jonas, A., Laschewsky, A. & Legras, R. Ultrathin polymer coatings by complexation of

polyelectrolytes at interfaces: suitable materials, structure, and properties. *Macromolecular rapid communications* **21**, 319-348 (2000).

17. Decher, G. Fuzzy nanoassemblies: toward layered polymeric multicomposites. *Science* **277**, 1232 (1997).

18. Hammond, P. Recent explorations in electrostatic multilayer thin film assembly. *Current Opinion in Colloid & Interface Science* **4**, 430-442 (1999).

19. Schlenoff, J. & Dubas, S. Mechanism of polyelectrolyte multilayer growth: Charge overcompensation and distribution. *Macromolecules* **34**, 592-598 (2001).

20. Schwarz, S., Eichhorn, K., Wischerhoff, E. & Laschewsky, A. Polyelectrolyte adsorption onto planar surfaces: a study by streaming potential and ellipsometry measurements. *Colloids and Surfaces A: Physicochemical and Engineering Aspects* **159**, 491-501 (1999).

21. Okubo, T. & Suda, M. Absorption of polyelectrolytes on colloidal surfaces as studied by electrophoretic and dynamic light-scattering techniques. *Journal of colloid and interface science* **213**, 565-571 (1999).

22. Yoo, D., Shiratori, S. & Rubner, M. Controlling bilayer composition and surface wettability of sequentially adsorbed multilayers of weak polyelectrolytes. *Macromolecules* **31**, 4309-4318 (1998).

23. Shiratori, S. & Rubner, M. pH-dependent thickness behavior of sequentially adsorbed layers of weak polyelectrolytes. *Macromolecules* **33**, 4213-4219 (2000).

24. Mandel, M. & Leyte, J. Titration equation of weak polyacids. *Electroanalytical chemistry and interfacial electrochemistry* **37**, 297-301 (1972).

25. Overbeek, J. The dissociation and titration constants of polybasic acids. *Bull Soc Chim Belg* **57**, 252-261 (1948).

26. Schoch, R.B., Han, J. & Renaud, P. Transport phenomena in nanofluidics. *Reviews of Modern Physics* **80**, 839 (2008).

27. Mijatovic, D., Eijkel, J. & Berg, A. Technologies for nanofluidic systems: top-down vs. bottom-up—a review. *Lab on a Chip* **5**, 492-500 (2005).

28. Mao, P. & Han, J. Massively-parallel ultra-high-aspect-ratio nanochannels as mesoporous membranes. *Lab on a Chip* **9**, 586-591 (2009).

29. Jiang, H., Yoo, K., Yeh, J., Li, Z. & Tien, N. Fabrication of thick silicon dioxide sacrificial and isolation blocks. *Journal of Micromechanics and Microengineering* **12**, 87-95 (2002).

30. Mao, P. & Han, J. Fabrication and characterization of 20 nm planar nanofluidic channels by glass–glass and glass–silicon bonding. *Lab on a Chip* **5**, 837-844 (2005).

31. Lin, C., Lee, G., Lin, Y. & Chang, G. Fabrication of microfluidic systems on soda-lime glass. *Journal of Micromechanics and Microengineering* **11**, 726-732 (2001).

32. Fan, Z. & Harrison, D. Micromachining of capillary electrophoresis injectors and separators of glass

chips and evaluation of flow at capillary intersections. *Analytical chemistry(Washington, DC)* **66**, 177-184 (1994).

33. Harrison, D.J., Manz, A., Fan, Z., Luedi, H. & Widmer, H.M. Capillary electrophoresis and sample injection systems integrated on a planar glass chip. *Analytical Chemistry* **64**, 1926-1932 (1992).

34. Kim, P., Jeong, H., Khademhosseini, A. & Suh, K. Fabrication of non-biofouling polyethylene glycol micro-and nanochannels by ultraviolet-assisted irreversible sealing. *Lab on a Chip* **6**, 1432-1437 (2006).

35. Hadjichristidis, N., Pispas, S. & Floudas, G. *Block copolymers: synthetic strategies, physical properties, and applications*, (Wiley-Interscience, 2003).

36. Discher, D. & Eisenberg, A. Polymer vesicles. *Science* **297**, 967 (2002).

37. Satturwar, P., Eddine, M., Ravenelle, F. & Leroux, J. pH-responsive polymeric micelles of poly (ethylene glycol)-b-poly (alkyl (meth) acrylate-co-methacrylic acid): Influence of the copolymer composition on self-assembling properties and release of candesartan cilexetil. *European journal of pharmaceutics and biopharmaceutics* **65**, 379-387 (2007).

38. Bromberg, L. & Ron, E. Temperature-responsive gels and thermogelling polymer matrices for protein and peptide delivery. *Advanced drug delivery reviews* **31**, 197-221 (1998).

39. Agheli, H., Malmstrom, J., Larsson, E., Textor, M. & Sutherland, D. Large area protein nanopatterning for biological applications. *Nano Lett* **6**, 1165-1171 (2006).

40. Barbulovic-Nad, I., *et al.* Bio-microarray fabrication techniques-A review. *Critical reviews in biotechnology* **26**, 237-259 (2006).

41. Shim, H., *et al.* Patterning of proteins and cells on functionalized surfaces prepared by polyelectrolyte multilayers and micromolding in capillaries. *Biosensors and Bioelectronics* **22**, 3188-3195 (2007).

42. Rusmini, F., Zhong, Z. & Feijen, J. Protein immobilization strategies for protein biochips. *Biomacromolecules* **8**, 1775-1789 (2007).

43. Dechesne, A., *et al.* A novel method for characterizing the microscale 3D spatial distribution of bacteria in soil. *Soil Biology and Biochemistry* **35**, 1537-1546 (2003).

44. Young, I. & Crawford, J. Interactions and self-organization in the soil-microbe complex. *Science* **304**, 1634 (2004).

45. Grundmann, G., *et al.* Spatial modeling of nitrifier microhabitats in soil. *Soil Science Society of America Journal* **65**, 1709 (2001).

46. Nunan, N., Wu, K., Young, I., Crawford, J. & Ritz, K. Spatial distribution of bacterial communities and their relationships with the micro-architecture of soil. *FEMS microbiology ecology* **44**, 203-215 (2003).

47. Letters, E. The metacommunity concept: a framework for multi-scale community ecology. *Ecology Letters* **7**, 601-613 (2004).

48. Treves, D., Xia, B., Zhou, J. & Tiedje, J. A two-species test of the hypothesis that spatial isolation influences microbial diversity in soil. *Microbial ecology* **45**, 20-28 (2003).

49. Tilman, D. & Kareiva, P. *Spatial ecology: the role of space in population dynamics and interspecific interactions*, (Princeton Univ Pr, 1997).

50. Tilman, D. *Resource competition and community structure*, (Princeton Univ Pr, 1982).

51. Ginger, D., Zhang, H. & Mirkin, C. The evolution of dip-pen nanolithography. *Angewandte Chemie-International Edition* **43**, 30-45 (2004).

52. Doraiswamy, A., Dunaway, T., Wilker, J. & Narayan, R. Inkjet printing of bioadhesives. *Journal of biomedical materials research. Part B, Applied biomaterials* **89**, 28 (2008).

53. Shin, D., *et al.* Protein patterning by maskless photolithography on hydrophilic polymer-grafted surface. *Biosensors and Bioelectronics* **19**, 485-494 (2003).

54. Schmalenberg, K., Buettner, H. & Uhrich, K. Microcontact printing of proteins on oxygen plasma-activated poly (methyl methacrylate). *Biomaterials* **25**, 1851-1857 (2004).

55. Olle, E., *et al.* Comparison of antibody array substrates and the use of glycerol to normalize spot morphology. *Experimental and molecular pathology* **79**, 206-209 (2005).

56. Zhu, H. & Snyder, M. Protein arrays and microarrays. *Current Opinion in Chemical Biology* **5**, 40-45 (2001).

57. Tan, J., Tien, J. & Chen, C. Microcontact printing of proteins on mixed self-assembled monolayers. *Langmuir* **18**, 519-523 (2002).

58. Blawas, A. & Reichert, W. Protein patterning. *Biomaterials* **19**, 595-609 (1998).

59. Flounders, A., Brandon, D. & Bates, A. Patterning of immobilized antibody layers via photolithography and oxygen plasma exposure. *Biosensors and Bioelectronics* **12**, 447-456 (1997).

60. Krishnan, S., Weinman, C. & Ober, C. Advances in polymers for anti-biofouling surfaces. *Journal of Materials Chemistry* **18**, 3405-3413 (2008).

61. Quinn, A., Tjipto, E., Yu, A., Gengenbach, T. & Caruso, F. Polyelectrolyte blend multilayer films: Surface morphology, wettability, and protein adsorption characteristics. *Langmuir* **23**, 4944-4949 (2007).

62. Shim, H., Lee, J., Kim, B., Son, Y. & Lee, C. Facile Preparation of Biopatternable Surface for Selective Immobilization from Bacteria to Mammalian Cells. *Journal of Nanoscience and Nanotechnology* **9**, 1204-1209 (2009).

63. Hammond, P. Form and function in multilayer assembly: new applications at the nanoscale. *Advanced Materials* **16**, 1271-1293 (2004).

64. Tang, Z., Wang, Y., Podsiadlo, P. & Kotov, N. Biomedical applications of layer-by-layer assembly: from biomimetics to tissue engineering. *Advanced Materials* **19**, 906-908 (2007).

65. Liu, Y., *et al.* Synthesis, stability, and cellular internalization of gold nanoparticles containing mixed

peptide-poly (ethylene glycol) monolayers. *Anal. Chem* **79**, 2221–2229 (2007).

66. Park, S., Yang, H., Kim, D., Jo, K. & Jon, S. Rational design of amphiphilic polymers to make carbon nanotubes water-dispersible, anti-biofouling, and functionalizable. *Chemical Communications* **2008**, 2876-2878 (2008).

67. Krishnan, S., *et al.* Anti-biofouling properties of comblike block copolymers with amphiphilic side chains. *Langmuir* **22**, 5075-5086 (2006).

68. Vermette, P. & Meagher, L. Interactions of phospholipid-and poly (ethylene glycol)-modified surfaces with biological systems: relation to physico-chemical properties and mechanisms. *Colloids and Surfaces B: Biointerfaces* **28**, 153-198 (2003).

69. Spencer, J., Bodner, G., Rickard, L. & Schmidkonz, B. *Chemistry: structure and dynamics*, (John Wiley).